Atmospheric
Measurement
Techniques

Carbon monoxide total columns from SCIAMACHY 2.3 μm atmospheric reflectance measurements: towards a full-mission data product (2003–2012)

T. Borsdorff[1], **P. Tol**[1], **J. E. Williams**[2], **J. de Laat**[2], **J. aan de Brugh**[1], **P. Nédélec**[3], **I. Aben**[1], **and J. Landgraf**[1]

[1]SRON Netherlands Institute for Space Research, Utrecht, the Netherlands
[2]Royal Netherlands Meteorological Institute (KNMI), de Bilt, the Netherlands
[3]Laboratoire d'aérologie (LA), CNRS UMR-5560 et Observatoire Midi-Pyrénées, Université Paul-Sabatier, Toulouse, France

Correspondence to: T. Borsdorff (t.borsdorff@sron.nl)

Abstract. We present a full-mission data product of carbon monoxide (CO) vertical column densities using the 2310–2338 nm SCIAMACHY reflectance measurements over clear-sky land scenes for the period January 2003–April 2012. The retrieval employs the SICOR algorithm, which will be used for operational data processing of the Sentinel-5 Precursor mission. The retrieval approach infers simultaneously carbon monoxide, methane and water vapour column densities together with a Lambertian surface albedo from individual SCIAMACHY measurements employing a non-scattering radiative transfer model. To account for the radiometric instrument degradation including the formation of an ice-layer on the 2.3 μm detector array, we consider clear-sky measurements over the Sahara as a natural calibration target. For these specific measurements, we spectrally calibrate the SCIAMACHY measurements and determine a spectral radiometric offset and the width of the instrument spectral response function as a function of time for the entire operational phase of the mission. We show that the smoothing error of individual clear-sky CO retrievals is less than ±1 ppb and thus this error contribution does not need to be accounted for in the validation considering the much higher retrieval noise. The CO data product is validated against measurements of ground-based Fourier transform infrared spectrometers at 27 stations of the NDACC-IRWG and TCCON network and MOZAIC/IAGOS aircraft measurements at 26 airports worldwide. Overall, we find a good agreement with TCCON measurements with a mean bias

$\bar{b} = -1.2$ ppb and a station-to-station bias with $\overline{\sigma} = 7.2$ ppb. The negative sign of the bias means a low bias of SCIA-MACHY CO with respect to TCCON. For the NDACC-IRWG network, we obtain a larger mean station bias of $\bar{b} = -9.2$ ppb with $\overline{\sigma} = 8.1$ ppb and for the MOZAIC/IAGOS measurements we find $\bar{b} = -6.4$ ppb with $\overline{\sigma} = 5.6$ ppb. The SCIAMACHY data set is subject to a small but significant bias trend of 1.47 ± 0.25 ppb yr^{-1}. After trend correction, the bias with respect to MOZAIC/IAGOS observation is 2.5 ppb, with respect to TCCON measurements it is -4.6 ppb and with respect to NDACC-IRWG measurements -8.4 ppb. Hence, a discrepancy of 3.8 ppb remains between the global biases with NDACC-IRWG and TCCON, which is confirmed by directly comparing NDACC-IRWG and TCCON measurements. Generally, the scatter of the individual SCIA-MACHY CO retrievals is high and dominated by large measurement noise. Hence, for practical usage of the data set, averaging of individual retrievals is required. As an example, we show that monthly mean SCIAMACHY CO retrievals, averaged separately over Northern and Southern Africa, reflect the spatial and temporal variability of biomass burning events in agreement with the global chemical transport model TM5.

1   Introduction

Carbon monoxide (CO) is an important atmospheric trace gas for the understanding of tropospheric chemistry and air quality. Its main source is incomplete combustion of fossil fuel and biomass and the oxidation of atmospheric methane and other hydrocarbons. The reaction of CO with the hydroxyl radical (OH) represents its major atmospheric sink and thus CO regulates the self-cleaning capability of the atmosphere (Spivakovsky et al., 2000). Enhanced CO concentration can indicate anthropogenic air pollution (Logan et al., 1981) and as a precursor of ozone (O_3) formation it influences tropospheric air quality (Seiler and Fishman, 1981). Moreover, by constraining the depletion of methane (CH_4), CO affects indirectly global warming (Daniel and Solomon, 1998) and due to its moderately long lifetime of several weeks to several months (Holloway et al., 2000), it is a tracer for global transport and redistribution of pollutants in the atmosphere (e.g. Yurganov et al., 2004, 2005; Gloudemans et al., 2006).

Since 2000, the global concentration of CO has been measured by various satellite missions. For example, the MO-PITT (Measurements of Pollution in the Troposphere) instrument uses the spectral measurements at 2.3 and 4.7 μm to retrieve CO (Deeter et al., 2003). AIRS (Atmospheric Infrared Sounder; McMillan et al., 2005), launched in 2002 onboard the Aqua satellite, TES (Tropospheric Emission Spectrometer; Rinsland et al., 2006) and IASI (Infrared Atmospheric Sounding Interferometer; Turquety et al., 2004), onboard of a series of three METOP (Meteorological Operational) satellites, employ spectral measurements at 4.7 μm to infer atmospheric CO abundances. The Scanning Imaging Absorption Spectrometer for Atmospheric Cartography (SCIAMACHY) was one of the first space-based instruments observing CO from the shortwave infrared (SWIR) range around 2.3 μm (Bovensmann et al., 1999) and it was fully operational from January 2003 until April 2012 when contact with its host EN-VISAT (Environmental Satellite) was lost. In this period, an almost continuous long-term record of more than 9 years of SWIR measurements in the 2.3 μm spectral range from space was recorded. For cloud-free scenes, these spectra are sensitive to the total column density of CO with a good vertical sensitivity throughout the whole atmosphere (Buchwitz et al., 2004; Gloudemans et al., 2008).

In recent years, several algorithms have been developed to infer CO total columns from SCIAMACHY's SWIR measurements – e.g. IMAP-DOAS (Iterative Maximum A Posteriori Differential Optical Absorption Spectroscopy; Frankenberg et al., 2005), WFM-DOAS (Weighting Function Modified Differential Optical Absorption Spectroscopy; Buchwitz et al., 2004), IMLM (Iterative Maximum Likelihood Method; Gloudemans et al., 2009), and the operational SCIAMACHY CO processor (Gimeno García et al., 2011). The global CO fields were used for a range of applications – e.g. the detection of biomass burning events (Buchwitz et al., 2004), to study the inter-annual variability of CO on the global scale

(Gloudemans et al., 2009), to investigate pollution patterns of megacities (Buchwitz et al., 2007) and the long-range transport of CO in the Southern Hemisphere (Gloudemans et al., 2009), which indicates the broad scope of application for this data product. Furthermore, the SCIAMACHY CO measurements were compared with corresponding MOPITT CO retrievals (de Laat et al., 2010a) and additionally validated with CO observations of ground-based spectrometers (de Laat et al., 2010b) and MOZAIC/IAGOS aircraft measurements (de Laat et al., 2012). All these previous studies were dedicated to the early years of the mission before 2009. A possible reason for this is the extensive degradation of the instrument (Gloudemans et al., 2008), caused by the growing ice layer on the detector array and a considerable loss of detector pixels due to radiation damage in the later years of the mission. This reduces the radiometric quality of the SCIAMACHY spectra, which seriously complicates the processing of a SCIAMACHY CO product for the entire mission period.

The Tropospheric Monitoring Instrument (TROPOMI) on board of the Sentinel 5 Precursor (SP-5) mission is expected to be launched in 2016. TROPOMI covers the same 2.3–2.4 μm spectral range as SCIAMACHY with the same spectral resolution but with an improved radiometric performance and a better spatial resolution of the TROPOMI instrument. For the S5-P mission, the highly efficient Shortwave Infrared Carbon Monoxide Retrieval algorithm (SICOR) (Vidot et al., 2012) was developed to meet the demanding requirements of operational data processing regarding calculation time. In this study, we apply the SICOR algorithm to the SWIR measurements of the SCIAMACHY instrument and infer a data set of CO vertical columns for the entire ENVISAT mission (2003–2012), limited to land and cloud-free scenes. This study represents the first application of the TROPOMI operational processor to real data.

Due to unexpected in-orbit problems of the SCIAMACHY measurements in the 2.3 μm spectral range (Gloudemans et al., 2005), recalibration of the radiometric measurements is needed. For this purpose, we use clear-sky measurements over the Sahara as a natural calibration target in combination with accurate a priori knowledge of the atmospheric methane abundances in this region. For the entire mission lifetime, we determine the temporal dependence of the spectral calibration, a spectral radiometric offset, and the width of the instrument spectral response function from these measurements. Furthermore, we use SCIAMACHY's solar measurements to obtain a proper reflectance retrieval. Here, multiplicative radiometric errors common to both the radiance and irradiance measurement cancel out and are thus not relevant for the retrieval. Finally, the CO data set is validated with ground-based measurements of the TCCON (Total Carbon Column Observing Network) and NDACC-IRWG (Network for the Detection of Atmospheric Composition Change – Infrared Working Group) at 27 sites and aircraft measurements close to 26 airports of the MOZAIC (Measurement of Ozone

and Water Vapour on Airbus in-service Aircraft) and IAGOS (In-service Aircraft for a Global Observing System) project.

Averaging of individual SCIAMACHY CO retrievals is essential for data usage to reduce the retrieval noise to an acceptable level. The required degree of averaging depends on the properties of the considered ground scene and the measurement geometry of the instrument. To illustrate potential data use, we compare the spatial and temporal variation of SCIAMACHY CO fields over biomass burning areas in Africa with model fields of a global chemistry transport model (TM5). Choosing an appropriate balance between temporal and spatial averaging of individual SCIAMACHY retrievals allows us to obtain useful information about the atmospheric CO concentration.

For the first six years of the mission, our SCIAMACHY CO data set compares well with previous work by de Laat et al. (2010b), which becomes obvious when comparing the validation of the data sets with collocated ground-based Fourier transform infrared spectroscopy (FTIR) measurements. The retrieval noise statistics in the early years of the mission are comparable but the resulting CO time series of the new data set is more homogeneous due to our calibration approach. Moreover, the main achievement of this study is that a valuable CO data product is provided for the years after 2008 considering the advanced degradation of the SCIA-MACHY instrument in that period. Furthermore, the southern hemispheric bias mentioned by de Laat et al. (2010b) is significantly reduced.

The paper is organised as follows: Sect. 2 summarises the inversion approach and in Sect. 3 we discuss the degradation of SCIAMACHY instrument and propose a mitigation approach. The validation of the CO data product against NDACC-IRWG, TCCON and MOZAIC/IAGOS measurements discussed in Sects. 4 and 5 illustrates potential data usage showing a comparison with CO model fields that are simulated by the TM5 global chemistry transport model. Finally, Sect. 6 summarises and concludes the paper.

2 Retrieval approach

To obtain CO vertical column densities, we use SCIA-MACHY SWIR measurements in the spectral range 2310.7–2338.4 nm with a spectral resolution of 0.2 nm and a spectral sampling distance of 0.1 nm. The retrieval is based on the profile scaling approach, which was first applied by Gloude-mans et al. (2008) to interpret SCIAMACHY data. The approach is discussed in detail by Borsdorff et al. (2014) and this section summarises its main characteristics.

Basically, the retrieval approach scales an n-dimensional reference profile ρ_{ref}, which is the input to a radiative transfer model, to fit SCIAMACHY reflectance measurements. Hence, ρ_{ref} describes the vertical concentration of an atmospheric trace gas in arbitrary units. Subsequently, we estimate the retrieved CO vertical column density c by

$$c = \boldsymbol{C}^T \alpha \boldsymbol{\rho}_{ref}, \tag{1}$$

with the profile scaling factor α. Here, the n-dimensional vector $\boldsymbol{C} = (f_1, \ldots, f_n)$ approximates the vertical integration, where f_k converts the kth element of the state vector to the corresponding partial column amount of the trace gas. For the sake of simplicity, we refer to the retrieval of the total column density c when meaning this approach in the following.

For the inversion, a forward model $\boldsymbol{F}$ is needed, which describes the m-dimensional measurement $\boldsymbol{y}_{meas}$ within the spectral error $\boldsymbol{e}_y$, namely

$$\boldsymbol{y}_{meas} = \boldsymbol{F}(\boldsymbol{x}, \boldsymbol{b}) + \boldsymbol{e}_y. \tag{2}$$

Here, state vector $\boldsymbol{x}$ contains all parameters to be retrieved including the column density of CO and other trace gases. The forward model vector $\boldsymbol{b}$ includes all parameters which are needed for the simulation but are assumed to be known a priori. For the measurement, we employ a non-scattering radiative transfer model (Vidot et al., 2012) which simulates atmospheric transmission including Lambertian reflection at the Earth surface. Figure 1 shows a typical transmission spectrum in the retrieval window for clear-sky conditions and the individual spectral contributions of the trace gases HDO, CO, H_2O and CH_4. The forward model employs the cross-section database by Gloudemans et al. (2009), which comprises CO and CH_4 absorption cross-sections from the high-resolution transmission molecular absorption database (HI-TRAN) Rothman et al. (2005) and Predoi-Cross et al. (2006), respectively, and H_2O and HDO cross sections from Jenou-vrier et al. (2007). The spectral fit window is extended significantly with respect to the window used by Gloudemans et al. (2008) to establish a stable retrieval for the entire mission period. This is particularly important for the later years of the mission with a significant loss of spectral pixels of the SCIAMACHY channel 8 detector due to radiation damage. The selected window includes strong absorption lines of CH_4 between 2315 and 2320 nm and a nearly translucent range in the range 2310–2315 nm. Both spectral features are needed to mitigate the degradation of the instrument by fitting effective instrument parameters as described in the following section.

To invert Eq. (2), we employ a Gauss–Newton iteration scheme where the forward model $\boldsymbol{F}$ is linearised each iteration step around the solution $\boldsymbol{x}_0$ of the previous iteration. Thus, we can rewrite Eq. (2) as

$$\boldsymbol{y} = \mathbf{K}\boldsymbol{x} + \boldsymbol{e}_y \tag{3}$$

with $\boldsymbol{y} = \boldsymbol{y}_{meas} - \boldsymbol{F}(\boldsymbol{x}_0) + \mathbf{K}\boldsymbol{x}_0$ and the Jacobian or kernel matrix $\mathbf{K} = \partial \boldsymbol{F}/\partial \boldsymbol{x}(\boldsymbol{x}_0)$. Subsequently, Eq. (2) is inverted by minimising the least squares cost function

$$\boldsymbol{x}_{ret} = \min_{\boldsymbol{x}} \left\{ \|\mathbf{S}_y^{-1/2}(\mathbf{K}\boldsymbol{x} - \boldsymbol{y})\|_2^2 \right\}, \tag{4}$$
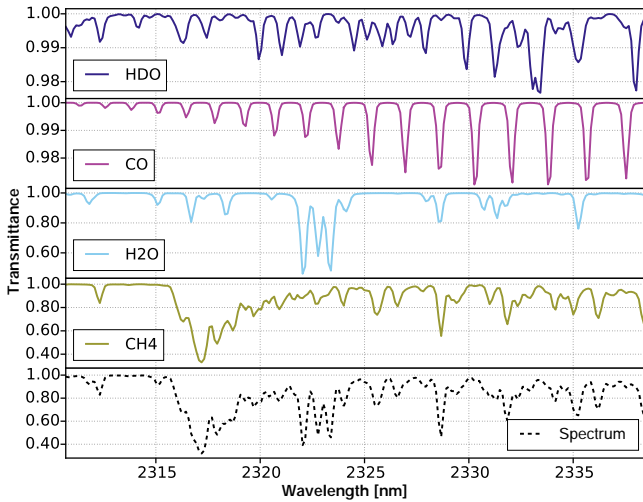
Figure 1. Simulation of atmospheric transmission spectra between 2310.7 and 2338.3 nm with a spectral resolution of 0.25 nm using HITRAN 2008 spectroscopy (Rothman et al., 2003). Panel 1–4: individual atmospheric absorptions of HDO, CO, H_2O and CH_4. Lower panel: total atmospheric transmission.

where $\| \cdot \|_2$ represents the L_2 norm and $\mathbf{S}_y \in \mathbb{R}^{m \times m}$ is the non-singular measurement error covariance matrix. Simultaneously with CO, we retrieve the vertical column densities of HDO, H_2O and CH_4 from the SWIR measurements using per species the explained profile scaling approach. Additionally, we infer a wavelength-dependent albedo described by a quadratic polynomial with respect to wavelength. The solution of Eq. (4) can be expressed by the gain matrix $\mathbf{G}$:

$$x_{\text{ret}} = \mathbf{G} y \tag{5}$$

with

$$\mathbf{G} = \left(\mathbf{K}^T \mathbf{S}_y^{-1} \mathbf{K} \right)^{-1} \mathbf{K}^T \mathbf{S}_y^{-1}. \tag{6}$$

The retrieved vertical column density c_{ret} is an effective column product due to the regularisation inherent to the profile scaling approach. The relation between the effective column and the true atmospheric abundance is described by the total column averaging kernel $\mathbf{a}_{\text{col}}$:

$$c_{\text{ret}} = \mathbf{a}_{\text{col}} \boldsymbol{\rho}_{\text{true}} + e_{\text{c}}, \tag{7}$$

where e_{c} is the column retrieval error due to the measurement error e_y and $\boldsymbol{\rho}_{\text{true}}$ is the true trace gas profile. A numerically efficient algorithm to calculate $\mathbf{a}_{\text{col}}$ is presented in Borsdorff et al. (2014). The total column averaging kernel represents an altitude-weighted integration of the true profile taking into account the particular retrieval sensitivity. The differences between the true column, $c_{\text{true}} = \boldsymbol{C}^T \boldsymbol{\rho}_{\text{true}}$, and the effective column, $c_{\text{eff}} = \mathbf{a}_{\text{col}} \boldsymbol{\rho}_{\text{true}}$, cannot be inferred from the measurement and is also known as the null space or smoothing error of the retrieval (Borsdorff et al., 2014; Rodgers, 2000),

$$e_{\text{null}} = (\boldsymbol{C}^T - \mathbf{a}_{\text{col}}) \boldsymbol{\rho}_{\text{true}}. \tag{8}$$

Finally, we characterise the noise on the retrieval product due to the measurement noise, described by the retrieval noise covariance

$$\mathbf{S}_x = \mathbf{G} \mathbf{S}_y \mathbf{G}^T. \tag{9}$$

In this manner, we have defined all diagnostic tools for our retrieval. A detailed overview of the profile-scaling approach is given in Borsdorff et al. (2014).

The retrieval depends on a priori information, which is adopted from different sources. Surface pressure, temperature profiles and water vapour reference profiles (H_2O, HDO) are based on the ECMWF (The European Centre for Medium-Range Weather Forecasts) ERA-Interim (Re-Analysis Interim) data set, which is sampled every 6 h on 60 vertical layers and on a 0.75° latitude by 0.75° longitude grid (Dee et al., 2011). CO and CH_4 reference profiles are taken from 3-dimensional global chemistry transport simulations of TM5 covering the entire mission period (Williams et al., 2013, 2014), which includes seasonal and interannual variability of the a priori information on the relative CO profile. Atmospheric trace gas profiles are provided every 3 h on 34 layers and on a 2° latitude by 3° longitude grid. For every SCIAMACHY measurement, the model data are spatially resampled to the satellite ground pixel and interpolated in time. Moreover, we account for the differences between the mean SCIAMACHY pixel elevation and the mean pixel elevation of the model data. First, we calculate the mean SCIAMACHY pixel height using the digital Shuttle Radar Topography Mission (SRTM) elevation map with a spatial resolution of 15 arcsec (Farr et al., 2007) and subsequently, all model profiles are interpolated to the mean altitude of a SCIAMACHY ground pixel.

One may question the relevance of the null-space error and the need for column averaging kernels for a proper validation of our data product. Generally, the correct use of Eq. (7) requires measurements of the CO vertical profile. However, this hampers any validation of the SCIAMACHY CO data product because measurements of CO profiles are hardly available for the mission period. On the other hand, a direct comparison of ground-based measurements of the total CO column with our data product suffers from the null-space error. Borsdorff et al. (2014) showed from simulations that in the presence of clouds the null-space error can easily exceed 30 % of the CO total column. The error is much smaller for clear sky conditions, depending on the reference profile used for scaling. To estimate the null-space error, we consider simulated retrievals for a set of solar zenith angles between 20 and 70°. Here, we used the US standard atmosphere (NOAA, 1976) for the profiles of dry air density, pressure, water and CO. The CH_4 profile is adopted from the CAMELOT (Chemistry of the Atmosphere Mission Concepts and Sentinel Observations Techniques) European background model atmosphere (Levelt et al., 2009). The total column averaging kernels are shown in the left panel of Fig. 2. Subsequently, we investigate the null-space error due to the difference of 533
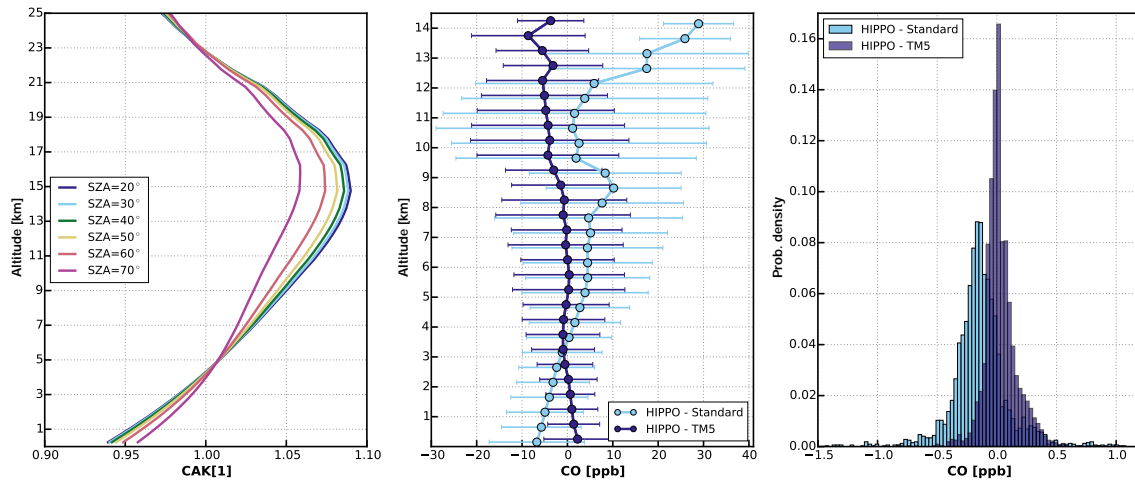
Figure 2. Left panel: SCIAMACHY CO total column averaging kernels for different solar zenith angles (SZAs). Middle panel: profile shape difference between HIPPO and TM5/US standard atmosphere. Right panel: probability density distribution of the null-space error.

CO profiles measured by the HIAPER Pole-to-Pole Observations (HIPPO) of the Carbon Cycle and Greenhouse Gases Study (Wofsy, 2011; Wofsy et al., 2012) and two different choices for the reference profiles. First, we consider the CO US standard profile and, second, we make use of the collocated CO profiles from the TM5 chemical transport model, which is the baseline of our algorithm. After scaling to the same total column, the variation of the HIPPO profiles and the corresponding reference profiles are shown in the middle panel of Fig. 2. Finally, the right panel of the figure shows the corresponding distribution of the null-space error utilising the column averaging kernels of the same figure. For both cases, the null-space error is less than 1 ppb (< 1 % of a mean CO total column) and so far less than the SCIAMACHY measurement noise error that varies between 30 ppb and > 170 ppb for individual retrievals (see Figs. 6 and 7).

Because of its randomness the noise error can be reduced by averaging multiple SCIAMACHY CO retrievals, which is not necessarily the case for the null space. However, a null-space error of the order of < 1 % for clear-sky SCIAMACHY CO retrievals represents a minor contribution to the overall error and is ignored in the following. So a direct comparison between ground-based measurements and SCIAMACHY retrievals is possible. Following this approach, strict cloud filtering of SCIAMACHY data is required. For this purpose, we employ the SCIAMACHY polarisation device (PMD) Identification of Clouds and Ice (SPICI) algorithm (Krijger et al., 2005).

3 Instrument calibration

In this section, we consider SCIAMACHY nadir measurements for the full operational phase of the mission from January 2003 to April 2012, where we use Level 1b spectra disseminated by ESA. The measurements are corrected for memory-nonlinearity and dark current using the Netherlands SCIAMACHY Data Center (NADC) toolbox Version 1.2 (http://www.sron.nl/~richardh/). Data recorded during SCIAMACHY's commissioning phase are not considered. The CO data processing relies on SCIAMACHY's forward scans for a solar zenith angle smaller than 80° and with a ground pixel size of about 30 km × 120 km (along-track × across-track) for an integration time of 0.5 s. At higher northern and southern latitudes the integration time is increased to 1 s, which accordingly doubles the across-track pixel size.

The SCIAMACHY detector in the 2.3–2.4 μm range (channel 8) suffers from detector radiation damage and very noisy detector pixels. Buchwitz et al. (2007) and Gloudemans et al. (2008) showed the severe sensitivity of CO retrievals to the instrument malfunction. A stable retrieval performance for the entire mission lifetime requires careful and strict spectral filtering of bad detector pixels based on in-flight detector performance monitoring. For measurements after 11 January 2005, we utilise the NADC version 3.0 time-dependent pixel mask, and for earlier measurements we fixed the pixel mask to that of this reference date. The channel 8 SCIAMACHY measurement noise is dominated by detector dark noise, which is estimated from SCIAMACHY's daily dark state measurements taken during the orbit eclipse.

Despite the strict filtering, the absolute radiometric calibration of SCIAMACHY Earthshine measurements is not accurate enough to retrieve CO. Figure 3 shows the time dependence of the mean solar signal. Besides the seasonal variation of the signal due to the change of the Earth–Sun distance throughout the year, the effect of the ice layer formation on the overall instrument transmission and the signal recovery due to the instrument heating during so-called decontami-
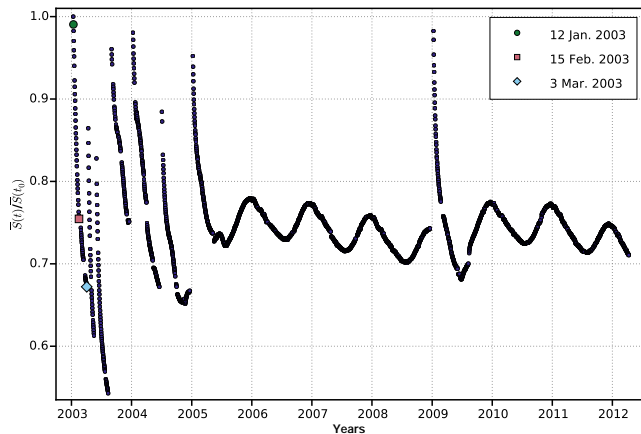
Figure 3. Mean signal of SCIAMACHY's daily sun mean reference (SMR) measurements (2288.72–2383.77 nm) as a function of time relative to 11 January 2003. Three example orbits are marked.

Table 1. Decontamination events of the SCIAMACHY instrument from 2003–2012. The dates are given together with the corresponding orbit ranges.

Number	Period	Orbits
1	1–4 Jan 2003	4380–4428
2	4–7 Apr 2003	5718–5766
3	21–25 May 2003	6384–6449
4	12–29 Aug 2003	7574–7827
5	18 Dec 2003–5 Jan 2004	9407–9673
6	18–30 Jun 2004	12 031–12 208
7	20 Dec 2004–5 Jan 2005	14 675–14 912
8	19 Dec 2008–7 Jan 2009	35 574–35 848

nation events (see Table 1) is clearly visible (Gloudemans et al., 2005). To mitigate effects on the CO data quality, our retrieval is based on the reflectance r_i, which is the ratio of the Earth radiance measurement I_i divided by the solar measurement S_i by the same detector pixel i, $r_i = I_i/S_i$. Here, we use SCIAMACHY's daily Sun mean reference measurements, determined from the Sun measurements via the elevation scan mirror. Subsequently, the solar measurements are interpolated to the measurement time of the Earthshine observation to account for a rapidly changing instrument directly after a thermal decontamination event.

The approach implies that any common multiplicative radiometric error of the Earth and solar observations cancels out in the reflectance ratio. However, any additive error component, e.g. due to detector hysteresis, non-linear radiometric detector response, dark detector current and analogue offset, still affects the radiometric accuracy of the reflectance spectrum and has to be accounted for by the radiometric calibration procedure.

Moreover, the use of SCIAMACHY reflectance measurements is hampered by the different malfunctioning pixels of the SCIAMACHY channel 8 detector for the Earthshine and solar observation mode. Filtering on both types of detector performance results in insufficient spectral coverage. To overcome this problem, we identify outliers in the solar irradiance spectrum and replace them by interpolated values. We start with a solar reference measurement $S(t_0, i)$ from 11 January 2003 (Fig. 4, upper panel), which is representative of a well-performing nearly ice-free detector (see Fig. 3). The nearly linear dependence of the solar signal on wavelength is due to the spectral variation of the detector pixel quantum efficiency. To detect spectral outliers, we determine the relative difference of the spectrum with respect to its running median spectrum, assuming an average over 1.4 nm. Differences between the original and spectrally smoothed solar spectrum

of $> 7\%$ are classified as outliers and are replaced by the smoothed value of the running median spectrum. Smaller differences are attributed to the pixel-to-pixel gain variation of the detector and the measurement noise and these features are maintained in the spectrum. This approach is based on the assumption that spectral variations in the solar spectrum in the considered spectral range are smooth.

In the following, we assume that the degradation of the solar spectrum can be described by

$$S_i(t) = \alpha(t) \cdot \beta_i(t) \cdot S_i(t_0) + \epsilon_i(t), \tag{10}$$

where α describes the relative degradation of the mean signal shown in Fig. 3, β represents the relative spectral degradation of detector pixel i and ϵ_i summarises high-frequency error contributions including noise and outliers. The middle panel of Fig. 4 shows the ratio $S_i(t)/(\alpha(t)S_i(t_0))$ for three exemplary days in the year 2003. Applying a 1.0 nm running median suppresses high-frequency contributions and allows us to estimate the degradation function β from the data. Subsequently, this defines also the error contribution $\epsilon_i(t)$ in Eq. (10), which can be used to detect spectral outliers in the solar measurement $S_i(t)$. Any measurement with $\epsilon_i(t) > 2\%$ is classified as an outlier and is replaced by the expected value $\alpha(t)\beta_i(t)S_i(t_0)$. In summary, the approach allows us to replace corrupted signals by interpolated values assuming a spectrally smooth degradation. High-frequency pixel-to-pixel variation present in the reference spectrum $S(t_o)$ are considered to be constant over the entire mission lifetime.

To account for an imperfect calibration resulting in an additive radiometric bias, we consider the Sahara region between 30 and 15° northern latitude and −15 and 30° longitude as a natural calibration target for the entire mission period. This region is chosen because of the high signal levels due to the high reflective desert surface, and because it is assured that the amount of CH_4 can be relatively well predicted using the TM5 model (Gloudemans et al., 2005). For measurements over this particular region, we modify our forward model by adding a polynomial expansion of an additive
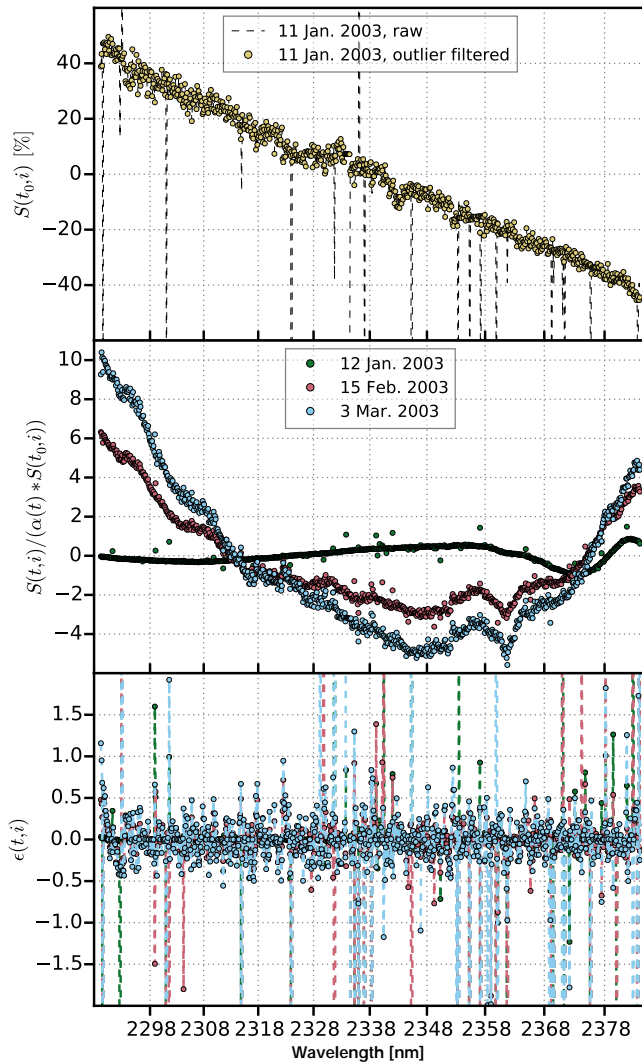
Figure 4. Upper panel: first SMR spectrum of 11 January 2003 expressed as the deviation from its mean signal This spectrum is used as reference in the following panels. Bad pixels were filtered and interpolated. Middle panel: SMR spectra for three example orbits divided by the reference and smoothed with a running median filter of 10 pixels half width. Lower panel: residuals of the smoothing.

radiometric bias,

$$F(x, b, a) = \hat{F}(x, b) + \sum_{i=0}^{3} a_i \cdot p_i(\lambda). \tag{11}$$

Here, $\hat{F}(x, b)$ denotes the forward calculation in Eq. (2), and p_i are Chebyshev polynomials as function of wavelength λ. The coefficients a_i can be determined as additional fit parameters of the retrieval algorithm because of the high radiometric signal over the desert region, where we fix the atmospheric methane abundance to the a priori model information. To fully exploit this approach, it was necessary to
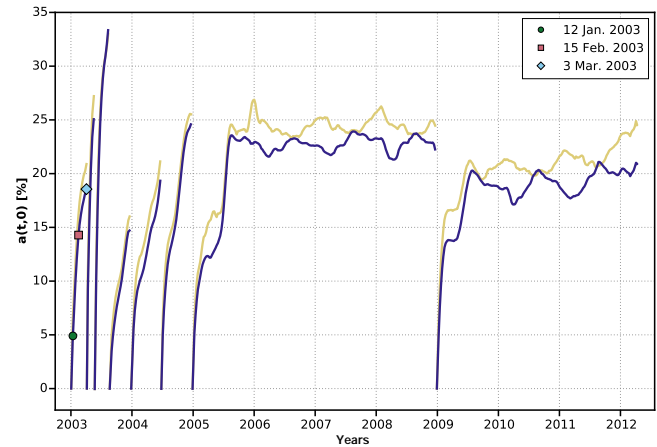
Figure 5. Zero-order radiometric offset over time retrieved from cloud-free high albedo SCIAMACHY spectra above the Sahara region (dark blue) and above Australia (yellow). The offset is given in percentage of the mean signal of the spectra and data gaps are interpolated. The three example orbits of Fig. 4 are marked.

include the strong CH_4 absorption between 2315–2320 nm in our spectral fitting window (see Fig. 1).

Figure 5 shows the temporal evolution of coefficient a_0, which represents a spectrally constant additive bias of the measurement. Here a_0 increases with a growing ice layer while the overall optical throughput of the instrument declines (see Fig. 3). For a fully established ice layer, the offset is 20–30 %. We attribute this offset to photons scattered in the ice layer and then detected at a spectrally shifted position on the detector. In other words, the effective spectral instrument response function is altered by the ice layer (Gloudemans et al., 2005). To account for this significant bias in our overall retrieval, we smooth the data over a 40-day period and correct all SCIAMACHY measurements accordingly. To demonstrate the general applicability of our approach to global data sets, we applied the same procedure for corresponding cloud-free measurements over Australia with a lower surface albedo and with different solar geometries. We obtained very similar radiometric biases (see Fig. 5) which supports the overall validity of the approach. The difference between the coefficients derived over Sahara and Australia (about 3 % in spring and in agreement in autumn) is not fully understood yet and is the topic of further investigation.

Subsequently, we evaluate the spectral calibration and the SCIAMACHY instrument spectral response function. Based on gas-cell measurements during the on-ground calibration of the instrument, Schrijver (1999, 2000b, 2001b) suggested using a quadratic polynomial in pixel number for the wavelength calibration for the channel 8 detector,

$$\lambda = a_0 + a_1 \cdot n + a_2 \cdot n^2, \tag{12}$$

where wavelength λ is given in nm and n denotes the spectral pixel number. For the purpose of this study, we adopted coefficients $a_1 = 0.135254$ nm and $a_2 = -1.19719 \times 10^{-5}$ nm from the previous studies but re-evaluated coefficient a_0 using the Sahara calibration scenes giving $a_0 = 2259.24$ nm.

Finally, we utilise the instrument spectral response function s as determined from pre-flight line source measurements (Schrijver, 2000a, 2001a),

$$s(n, n_0) = \frac{1}{N}$$
$$\cdot \left(b_0 \cdot \frac{b_1^2}{b_1^2 + (n - n_0)^2} + (1 - b_0) \cdot \frac{b_1^2}{b_1^2 + (n - n_0)^4} \right), \quad (13)$$

with $b_0 = 0.7532$, $b_1 = 0.4313$. N controls the overall normalisation of the response function and n denotes the pixel number, where n_0 represents the centre pixel. Substitution of Eq. (12) in Eq. (13) allows us to adjust the full width half maximum (FWHM) of the response function for the Sahara calibration scenes. Here, the FWHM varies between 0.19 and 0.24 nm which correlates with the growth of the detector ice-layer (not shown). However, since the effect on the CO retrieval was minor, we fixed the FWHM to a representative value of 0.21 nm.

4 Validation

To validate our SCIAMACHY CO data product, we have to treat two main problems. First, the retrieved CO column suffers severely from measurement noise. The retrieval noise error for low radiance signal can exceed 100 % of the retrieved column. Therefore, any validation can only be performed on quantities averaged in space and time. Second, a direct comparison with ground-based measurements is affected by representation errors. For example, a monthly mean CO concentration derived from ground-based measurements may differ from a corresponding monthly mean of SCIAMACHY measurements due to different temporal sampling. A strict temporal co-registration criterion for both ground-based and SCIAMACHY measurements may reduce the sampling effect but at the cost of fewer SCIAMACHY samplings, which in turn enhances the noise contribution. Both aspects have to be considered in an appropriate validation strategy of the SCIAMACHY CO data product.

4.1 Ground-based Fourier transform spectrometers

In this section, we validate the SCIAMACHY CO data product with the measurements of Fourier transform spectrometers used for observing CO column densities under clear-sky conditions allowing direct Sun measurements. Table 2 summarises the validation data set, which comprises measurements at various stations of the Infrared Working Group (IRWG) that is part of the Network for the Detection of Atmospheric Composition Change (NDACC, http://

www.ndsc.ncep.noaa.gov/) and of the TCCON (Wunch et al., 2010, 2011). The IRWG provides measurements in the mid-infrared with the aim of analysing the atmospheric composition of the troposphere and stratosphere. The NDACC-IRWG supplies CO total columns that we transformed to column mixing ratios by calculating air columns from the surface pressures at a station. At several sites, the data record covers the entire SCIAMACHY lifetime, and thus makes these data very suited for the validation of the SCIAMACHY data product. The TCCON network collects measurements in the same spectral range as recorded by SCIAMACHY from space. This results in a similar vertical sensitivity of both the SCIAMACHY and the TCCON product, which is in particular desirable for validation purposes (see e.g. Wunch et al., 2010, Fig. 3 and Borsdorff et al., 2014, Fig. 2). In 2004, TCCON started with the first instrument at Park Falls, WI, USA, and since then the network has grown gradually to 19 observation sites worldwide. Therefore, the TCCON data set is very well suited to validate SCIAMACHY measurements in the later years of the mission. This study is based on the TCCON GGG2014 data set (Deutscher et al., 2014; Wennberg et al., 2014c, e, a, b, d; Griffith et al., 2014a, b; Strong et al., 2014; Sussmann and Rettinger, 2014; Blumenstock et al., 2014; Kawakami et al., 2014; Sherlock et al., 2014; Warneke et al., 2014; Maziere et al., 2014; Kivi et al., 2014; Morino et al., 2014). Measurements at Ny-Ålesund, Bremen and Four Corners are taken from the GGG2012 data since those sites are not yet available in the 2014 data release.

To achieve the best quality of the SCIAMACHY data, we apply an a posteriori quality filter based on the following criteria:

1. The spectral fit residual χ^2 must be < 10.

2. The mean signal-to-noise ratio of the measurements in the fit window must be > 10.

3. The noise ϵ of the retrieved CO, CH_4 and H_2O column must be below an upper threshold, namely $\epsilon_{CO} < 1 \times 10^{19}$, $\epsilon_{CH_4} < 6 \times 10^{18}$, $\epsilon_{H_2O} < 2 \times 10^{22}$ molec cm^{-2}.

4. Only SCIAMACHY measurements are used, which are classified as cloud free by the SPICI algorithm.

Moreover, we selected SCIAMACHY measurements over land, which fall within a radius of 850 km around a TCCON or NDACC-IRWG station site. To derive one representative monthly value for both data sets, we interpolate the FTIR measurements to the point of the SCIAMACHY measurements at time t. For this purpose, we consider the ratio of the FTIR columns divided by the co-aligned TM5 columns at two adjacent FTIR samples, $\delta(t_1)$ and $\delta(t_2)$ at time t_1 and t_2. The temporal interpolated FTIR column $c^{FTIR}(t)$ is then given by

$$c^{FTIR}(t) = \delta(t) \cdot c^{TM5}(t), \quad (14)$$
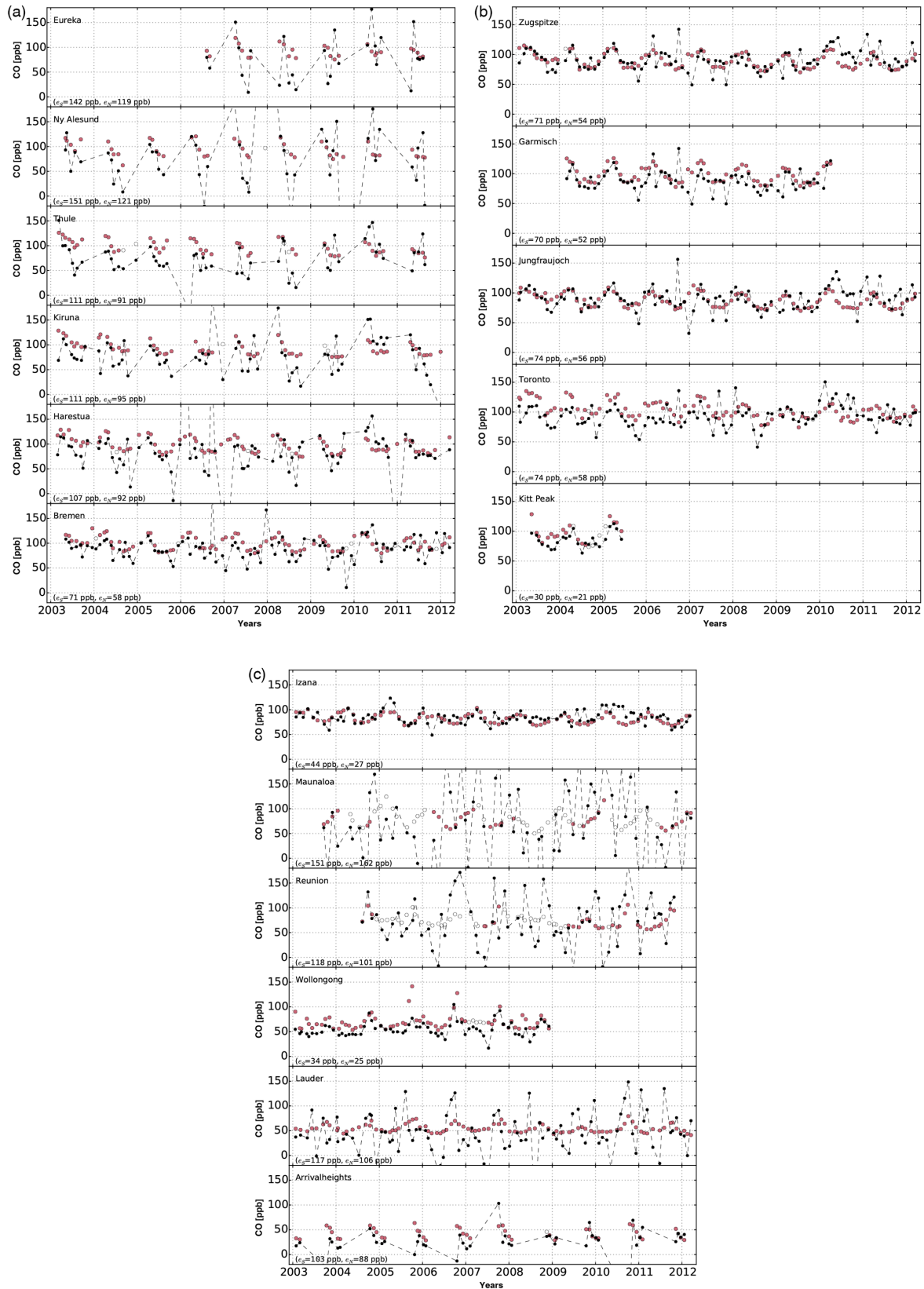
Figure 6. The 30-day medians of CO wet air column averaged mixing ratios measured by SCIAMACHY (black) and at various NDACC-IRWG stations (pink). To derive mixing ratios from the CO columns supplied by NDACC-IRWG we calculated total air columns from the surface pressure per station. Open circles denote interpolated values for periods where no NDACC-IRWG measurements are available.
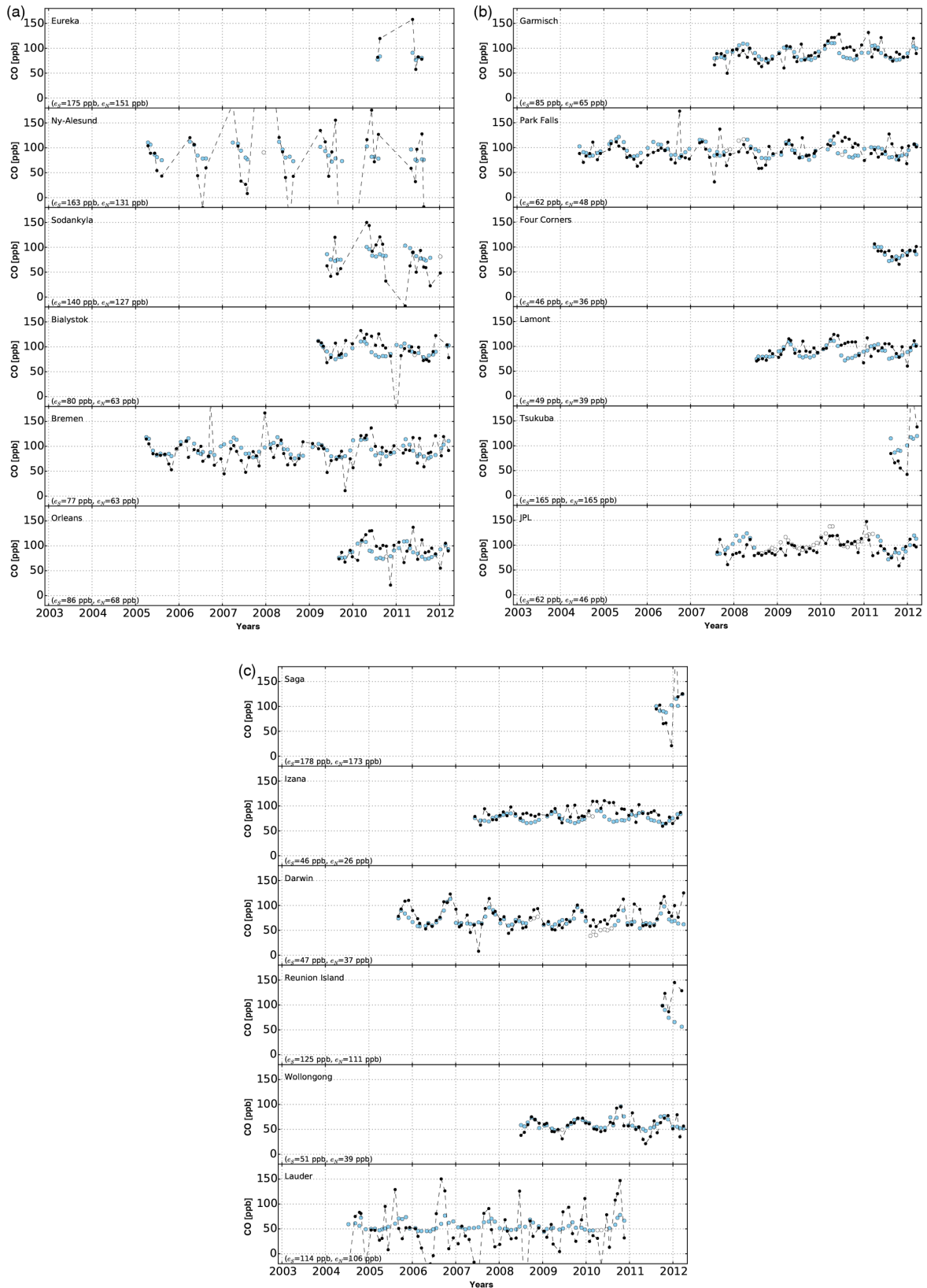
Figure 7. As Fig. 6, but for TCCON measurements indicated in blue. The GGG2014 release of TCCON was used but the stations Ny-Ålesund, Bremen and Four Corners are still based on GGG2012.
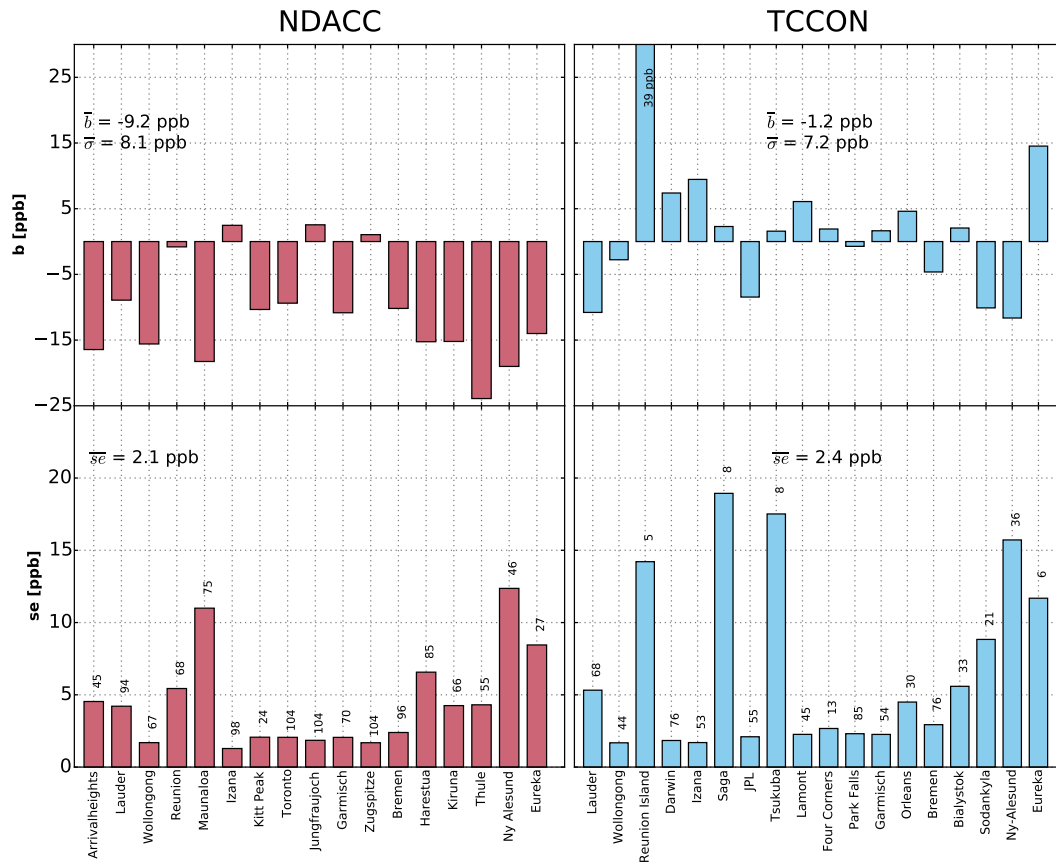
Figure 8. Mean bias (SCIAMACHY–FTS) between measurements of NDACC-IRWG (left panel) and TCCON (right panel) stations with collocated SCIAMACHY CO retrievals and the standard error of the mean bias derived from the 30 day median values shown in Figs. 6 and 7 (numbers of 30-day medians are indicated above bars). The $\bar{b}$ is the global mean bias (average of all station biases weighted by the standard error) and $\bar{\sigma}$ its standard deviation. $\hat{s}e$ is the average of all standard errors.

where $c^{\mathrm{TM5}}(t)$ is the corresponding TM5 CO column and $\delta(t)$ is the linear function through the adjacent points $\delta(t_1)$ and $\delta(t_2)$. Beforehand, we applied an additive bias correction to the TM5 model values such that the overall mean of the FTIR and TM5 values are the same. This simple interpolation scheme makes use of the precise FTIR measurement where the relative temporal trend in CO due to meteorology and photo-chemistry is adopted from the TM5 model. Subsequently, we correct $c^{\mathrm{FTIR}}(t)$ for differences between the surface elevation at the station site and the mean altitude of the individual satellite ground pixels using also TM5 CO profiles.

In this manner, we obtain two co-aligned data sets, which are subsequently used to derive monthly median CO column concentrations. The scattering of the individual SCIA-MACHY retrievals, which underlies each monthly median, is described by the half difference of the 15.9th and the 84.1th percentile e_S to be an analogue for the standard deviation of a normal distribution. For the same SCIAMACHY retrievals, we also calculate the mean retrieval noise e_N. To characterise the retrieval performance per station, we determine the

bias b as the mean difference between the monthly median CO concentrations of the ground-based and SCIAMACHY retrievals. A negative sign of a bias means that the SCIA-MACHY retrievals are biased low in comparison with the FTIR measurements. Moreover, we use the standard deviations σ of these difference and the standard error of the mean s_e to characterise the accuracy of b. Finally to characterise the overall performance, we determine the global mean bias $\bar{b}$ as the mean of the individual station biases weighted by their standard error s_e and the corresponding mean standard deviation $\bar{\sigma}$ and the mean standard error $\bar{s}_e$.

For all NDACC and TCCON stations in Table 2, Figs. 6 and 7 show time series of CO monthly median columns, and Fig. 8 summarises the validation diagnostics. Overall, the larger scatter of the individual SCIAMACHY CO columns is mainly caused by the large measurement noise indicated by the similar values of e_S and e_N. For some stations, e_N even exceeds a typical mean CO concentration, indicating the need to average data for validation purposes. For the sites Eureka, Ny-Ålesund, Sodankylä, Thule, Kiruna, Harestua, Mauna Loa, Reunion, Tsukuba, Saga and Lauder the noise in

Table 2. Ground-based FTIR stations used for validation. The latitude and longitude values are given in degrees, the surface elevation in km, and the overlap in time of the stations (NDACC-IRWG/TCCON) with SCIAMACHY in years.

Number	Name	Lat	Long	Alt	NDACC	TCCON
1	Eureka	80.05	−86.42	0.61	2006–2011	2010–2011
2	Ny-Ålesund	78.92	11.92	0.02	2003–2011	2005–2011
3	Thule	76.52	−68.77	0.22	2003–2011	–
4	Kiruna	67.84	20.40	0.42	2003–2011	–
5	Sodankylä	67.37	26.63	0.18	–	2009–2011
6	Harestua	60.20	10.80	0.60	2003–2012	–
7	Bialystok	53.23	23.03	0.16	–	2009–2012
8	Bremen	53.10	8.85	0.03	2003–2012	2005–2012
9	Orleans	47.97	2.11	0.13	–	2009–2012
10	Garmisch	47.48	11.06	0.75	2004–2010	2007–2012
11	Zugspitze	47.42	10.98	2.96	2003–2012	–
12	Jungfraujoch	46.55	7.98	3.58	2003–2012	–
13	Park Falls	45.94	−90.27	0.44	–	2004–2012
14	Toronto	43.66	−79.40	0.17	2003–2012	–
15	Four Corners	36.80	−108.48	1.64	–	2011–2012
16	Lamont	36.60	−97.49	0.32	–	2008–2012
17	Tsukuba	36.05	140.12	0.03	–	2011–2012
18	JPL	34.13	−118.13	0.21	–	2007–2012
19	Saga	33.24	130.29	0.01	–	2011–2012
20	Kitt Peak	31.90	−111.60	2.09	2003–2005	–
21	Izana	28.30	−16.48	2.37	2003–2012	2007–2012
22	Mauna Loa	19.54	−155.57	3.40	2003–2012	–
23	Darwin	−12.43	130.89	0.03	–	2005–2012
24	Reunion	−20.90	55.49	0.09	2004–2011	2011–2012
25	Wollongong	−34.41	150.88	0.03	2003–2008	2008–2012
26	Lauder	−45.05	169.68	0.37	2003–2012	2004–2010
27	Arrival heights	−77.82	166.65	0.20	2003–2012	–

the data is so large that monthly median values are still dominated by measurement noise. For the remaining stations, the scatter of the monthly median is reasonable, and for stations with a mean instrumental noise error $\bar{e}_N < 60$ ppb, the seasonal CO cycle becomes clearly visible in the SCIAMACHY time series. The high noise variability can be explained by a corresponding change of the mean signal strength because of varying surface albedo and solar zenith angle, both governing the amount of solar light reflected at the Earth surface.

Overall, Fig. 8 shows a good agreement between SCIAMACHY and TCCON ground-based measurements with a global bias of -1.2 ± 7.2 ppb. For some stations, we observe higher bias, e.g. at Reunion $b = 39$ ppb. These biases come along with large standard error due to a small number of measurements indicating a large uncertainty of b (see Fig. 7). For the NDACC-IRWG sites, we find a negative global bias $\bar{b} = -9.2 \pm 8.1$ ppb of the SCIAMACHY CO retrieval with respect to the NDACC-IRWG observations. Here, biases for mountain stations like Zugspitze, Jungfraujoch and Izana differ significantly from those at other sites. For the mountain sites, our correction for altitude differences between validation site and the SCIAMACHY ground pixel exceeds 50 % of the CO column and therefore our validation

is dominated by uncertainties of the TM5 model. The different global biases for TCCON and NDACC-IRWG measurements can be partly explained by the different temporal sampling of the validation sets combined with a small bias trend of $\bar{t} = 1.47 \pm 0.25$ ppb yr^{-1} in the SCIAMACHY CO columns, which we consider to be significant, keeping in mind both noise and a priori errors in the vertical shape of the reference profile scaled by the inversion (i.e. the null-space error) and the length of the time series. Figure 9 resolves this bias trend for seven NDACC-IRWG and TCCON stations, which cover the full SCIAMACHY mission period combined with low retrieval noise. The average bias trend $\bar{t}$ is calculated by an average of the individual bias trends weighted by their uncertainty, where we excluded measurements at Toronto because of a discontinuity of the NDACC-IRWG time series (see Fig. 6). This issue is already under investigation and does appear to be instrumental. When correcting the SCIAMACHY data for this bias trend, the bias with NDACC-IRWG becomes -8.4 ppb and with TCCON -4.6 ppb. Hence, a difference of 3.8 ppb remains between the TCCON and NDACC-IRWG validation. We consider this difference to be significant due to the small mean standard error $\bar{s}_e$ and we conclude that it is most probably caused by
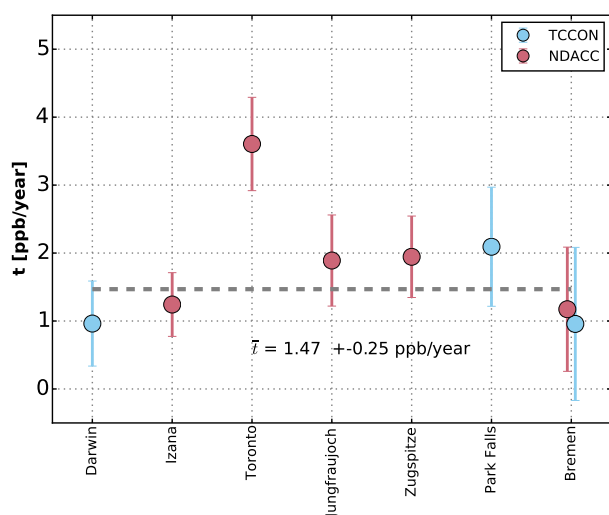
Figure 9. Linear bias trend t of the mean bias (SCIAMACHY–FTS) derived from 30-day median values shown in Figs. 6 and 7. Stations with a low retrieval noise that cover the full mission period were selected. Trends are given per station in ppb/year and error bars are the standard deviation. The $\hat{t}$ is the average of the bias trends weighted by the errors excluding measurements at Toronto.

a discrepancy between the TCCON and NDACC-IRWG retrievals. This is further confirmed by direct comparison of TCCON and NDACC-IRWG measurements performed at the same station.

4.2 MOZAIC/IAGOS aircraft measurements

Additionally, we validate the SCIAMACHY CO data product with CO total columns that are calculated from aircraft CO profile measurements supplied within the MOZAIC/IAGOS project. Since 1994, regular profile measurements of reactive gases by several long-distance passenger airliners were performed during ascent and descent phases (in total more than 40 000 flights). Aircraft descents and ascents are not strictly vertical profiles: the CO concentration at the surface is representative for the airports but the top of the height cruise can be far away from the take-off location. The representation error of the derived CO column for individual flight profile paths can reach up to 100 %, related to real spatiotemporal variability in CO total columns. However, Nédélec et al. (2003) indicated that the aircraft CO profile measurements reach a precision of about ±5 % and de Laat et al. (2014) showed that the errors caused by aircraft descent and ascent flight paths will average out for CO total columns when calculating the mean over longer time periods. However, biases due to highly polluted airports are still possible. Furthermore, the distance covered by the MOZAIC/IAGOS profiles used in this study is about 200–400 km and therefore is within the collocation area around the airports considered for the comparison with SCIAMACHY.

Table 3 summarises the validation data set, which comprises CO profile measurement at 26 airports worldwide. At many airports the data set covers the early years of the SCIA-MACHY mission and therefore forms a complement to the TCCON data set used in the previous section. More information about the MOZAIC/IAGOS programme and its data products is provided by Marenco et al. (1998) and Nédélec et al. (2015) and can be found at http://www.iagos.org/.

For the comparison with the SCIAMACHY CO retrieval, we only select MOZAIC/IAGOS profiles that reach at least 300 hPa and have measurements in every 100 hPa altitude bin. Above the maximum flight altitude, the profiles are extended using the Monitoring Atmospheric Composition and Climate (MACC) reanalysis data at 12:00 Coordinated Universal Time (UTC). MACC is pre-operational Copernicus Atmosphere Service, which provides data records of CO and other atmospheric trace gases (ozone, nitrogen oxides) as well as aerosols and covers the 10 years from 2003 to 2012 (Inness et al., 2013, 2015). The derived CO profiles are vertically integrated to obtain an estimate of the CO total columns. For comparison, individual SCIAMACHY retrievals are quality filtered a posteriori as described in Sect. 4.1. Because the MOZAIC/IAGOS data set is temporally more sparse than the ground-based FTIR data set in Sect. 4.1, we apply a slightly different collocation approach, proposed by de Laat et al. (2012). Here, SCIA-MACHY CO columns are spatially averaged within a $8° \times 8°$ ($\pm 4°$) area surrounding an airport location. Temporal averages are calculated around each MOZAIC/IAGOS sample, where the time window of averaging is chosen such that the retrieval noise of the average is equal to or smaller than 10^{17} molecules cm^{-2} (3.7 ppb). This yields a nonuniform sampling in time with samples of comparable retrieval noise.

We found that the MOZAIC/IAGOS measurements are on average biased low compared to the TM5 model used as priori for the SCIAMACHY CO retrieval (15 % ± 25 %). This bias is a general known chemistry-transport model issue. The difference between the MOZAIC/IAGOS measurements and the ECMWF MACC model used for extending the MOZAIC/IAGOS profiles is low (1 % ± 31 %). This is not surprising given that MACC ingests both MOPITT and IASI CO measurements in its data assimilation scheme.

Figure A1 shows time series of collocated SCIAMACHY and MOZAIC/IAGOS CO total columns for 26 airport locations with more than 13 collocations (similar to Figs. 6 and 7). Part of the data scatter is related to the spatiotemporal variability in CO. This affects both data sets differently, where SCIAMACHY samples represent an average for a larger area surrounding the airport, and MOZAIC/IAGOS columns are derived from slant profiles measured during descent and ascent of the aircraft over horizontal differences of 200–400 km. The good agreement of both data sets in their seasonal cycle is noticeable for Windhoek airport. Here, CO is subject to a strong seasonal cycle due to biomass burn-

Table 3. As Table 2, but for MOZAIC/IAGOS airports sites.

Number	Name	Lat	Long	Alt	MOZAIC/IAGOS
1	London	50.39	0.85	0.03	2006–2009
2	Frankfurt	50.32	7.71	0.11	2003–2011
3	Munich	48.85	12.70	0.45	2003–2011
4	Vienna	48.51	17.36	0.18	2003–2007
5	Portland	46.54	−122.18	0.02	2003–2009
6	Montreal	46.06	−72.65	0.04	2003–2006
7	Toronto	44.46	−78.59	0.17	2003–2011
8	Boston	43.01	−69.95	0.01	2003–2011
9	Chicago	42.79	−86.67	0.20	2003–2010
10	New York	41.23	−72.75	0.00	2003–2006
11	Beijing	40.38	115.22	0.04	2003–2005
12	Philadelphia	40.23	−74.23	0.01	2003–2006
13	Washington	39.94	−76.43	0.10	2004–2012
14	Tehran	35.98	50.24	1.01	2003–2005
15	Los Angeles	34.48	−117.47	0.04	2003–2005
16	Atlanta	34.43	−83.56	0.31	2003–2011
17	Dallas	33.83	−96.04	0.19	2003–2010
18	Tel Aviv	32.77	33.81	0.04	2003–2011
19	Cairo	30.72	31.15	0.12	2003–2011
20	Houston	30.63	−94.26	0.03	2003–2004
21	New Delhi	28.94	76.14	0.24	2003–2006
22	Kuwait City	28.74	48.44	0.06	2003–2004
23	Abu Dhabi	25.90	54.32	0.03	2003–2005
24	Hyderabad	17.54	77.40	0.63	2005–2011
25	Caracas	11.26	−66.37	0.07	2003–2009
26	Windhoek	−21.43	17.34	1.72	2005–2012

ing and the high surface albedo permits SCIAMACHY CO retrieval with a low instrument noise error. For airports like Beijing and Tehran, we notice high value outliers, where the MOZAIC/IAGOS columns are much larger than those measured by SCIAMACHY. This bias can be attributed to representation errors comparing localised pollution with spatial averages of SCIAMACHY CO observations. Overall, our results are in agreement with the findings of de Laat et al. (2012) analysing the SCIAMACHY CO measurements before 2009. Figure 10 summarises the comparison between SCIAMACHY and MOZAIC/IAGOS. We find a global bias of -6.4 ± 5.6 ppb. The difference between SCIAMACHY and MOZAIC/IAGOS shows a small but significant positive bias trend of 1.2 ± 0.7 ppb yr^{-1}, which is in agreement with Sect. 4.1. When correcting the SCIAMACHY data for this bias trend, the global bias reduces to 2.5 ppb which is in the range of the MOZAIC/IAGOS CO column uncertainty as reported by Nédélec et al. (2003).

5   Potential data application

One fundamental limitation of the SCIAMACHY CO data product is its large noise contribution. For most applications, individual CO columns must be averaged to reduce the retrieval noise to an acceptable level. The degree of averag-

ing depends on the signal-to-noise ratio of the corresponding SCIAMACHY observations and therefore on the brightness of the observed scenes. For example, for regions in Africa and Australia with high surface albedo, the retrieval noise is much lower than over dark scenes at high northern latitudes with low solar zenith angle. To mitigate this effect, one can consider data which are averaged both spatially and temporally. Averaging over the full-mission period (January 2003–April 2012), we obtain the CO global distribution shown in Fig. 11. This illustrates that a high spatial resolution can be achieved with the SCIAMACHY CO retrievals sacrificing temporal resolution. One of the most striking features of Fig. 11 is the enhanced CO column concentrations over central Africa due to biomass burning. To illustrate the seasonal variation of CO in this region, Fig. 12 shows the 30-day median of the SCIAMACHY CO concentration for northern hemispheric Africa (averaged between 0 and 10° latitude) and southern hemispheric Africa (averaged between 0 and −35° latitude). The figure also includes corresponding averages of TM5 model simulations which use the Global Fire Emissions Database (GFED) version 3 for the biomass burning input. Overall, the SCIAMACHY and TM5 fields agree well. The seasonal variation is present in both data sets including the phase shift between the northern and southern hemispheric CO concentration. In this case, the seasonal
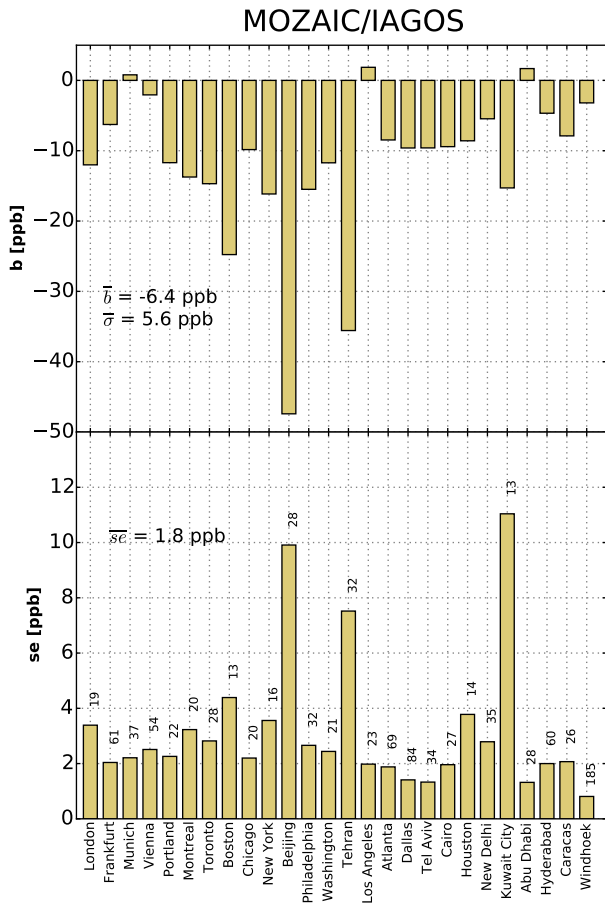
Figure 10. As Fig. 8, but for MOZAIC/IAGOS measurements.

variation of CO can be resolved with SCIAMACHY but at the cost of a poor spatial sampling.

Furthermore, we found that for sufficient signal level and temporal coverage, SCIAMACHY can catch the seasonal variability of the CO total column amount as reflected by NDACC-IRWG, TCCON and MOZAIC measurements. To demonstrate this, we calculated the Pearson coefficient between NDACC-IRWG, TCCON and MOZAIC measurements and the collocated and 30-day averaged SCIA-MACHY CO retrievals shown in Figs. 6, 7, and 10. For sites with a low CO retrieval noise error and a sufficient temporal coverage, we found a strong correlation showing that the seasonal variation is in agreement – e.g. for MOZAIC/IAGOS (0.7 for Windhoek and 0.8 for Los Angeles), for NDACC/IRWG (0.6 for Wollongong and 0.7 for Kitt Peak) and for TCCON (0.7 for Darwin and 0.7 for Wollongong).

This example illustrates nicely the limitations but also the strength of the presented SCIAMACHY CO data product. Clearly, the strength of the SCIAMACHY CO data product lies in the availability of more than 9 years continuous measurements but its limitation is its high retrieval noise. Hence, our recommendation for the use of the data set is to average

individual CO retrievals reducing the retrieval noise error to an acceptable level. Dependent on the considered application, this averaging can be performed spatially as well as temporarily. For example, 30-day means averaged spatially over 850 km are already sufficient for most sites worldwide. This is shown by the NDACC/TCCON validation in Sect. 4, where the SCIAMACHY CO retrieval showed a surprisingly homogeneous performance over the full mission time range. The SCIAMACHY CO data set must be seen as complementary to other measurements – e.g. of MOPITT (Deeter et al., 2003) – that provide a finer spatial and temporal resolution. Together with the future TROPOMI instrument, these missions will provide a unique long-term CO data set with global coverage from 2003 onward. In this context, a satellite inter-comparison of the CO retrieval from SCIAMACHY and MOPITT provides the perspective of an interesting and important follow-up study.

6 Summary and conclusions

We presented a full-mission data set of SCIAMACHY CO vertical column densities for cloud-free scenes over land. The retrieval employs the operational SICOR algorithm of the Sentinel-5 Precursor mission and is based on a profile scaling approach using SCIAMACHY 2.3 µm reflectance measurements. For the first time, a stable CO retrieval approach is presented for the entire mission period (January 2003– April 2012), which has to deal with the severe instrument degradation over the nearly 10-year mission period. While previous studies focused on the early years of the SCIA-MACHY mission period, we were able to mitigate effects of a changing instrument performance in space on the CO column product. For this purpose, we optimised the retrieval window to account for the serious loss of useful detector pixels caused by radiation damage. Furthermore, we estimated effective instrument parameters, which describe the temporal degradation of SCIAMACHY, using the Sahara region as a natural calibration target. These parameters describe the spectral calibration, a spectral radiometric offset, and the width of the instrument spectral response function. The CO total column amount is inferred simultaneously with methane and water vapour abundances and a Lambertian surface albedo from individual SCIAMACHY measurements assuming a non-scattering model atmosphere.

To obtain atmospheric CO abundances, the retrieval scales a CO reference profile, which represents a specific regularisation of the inversion. Consequently when interpreting the retrieved CO column as an estimate of the true column abundance, the data product suffers from a null-space error which describes the error in the inferred trace gas column due to the assumed profile to be scaled. Using 533 HIPPO CO profile measurements, we showed that for clear-sky conditions the null-space error is typically $< \pm 1$ ppb. This represents a minor error source and thus is not further considered in
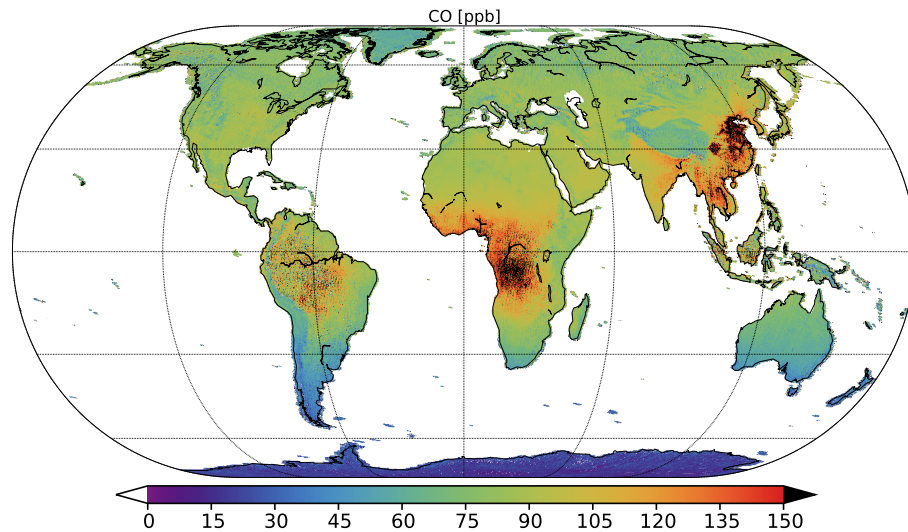
Figure 11. CO wet air column averaged mixing ratios over land and clear-sky scenes. The values are averaged from January 2003 to April 2012 on a cylindrical equal area projection with 180 grid points in latitude and 360 in longitude.
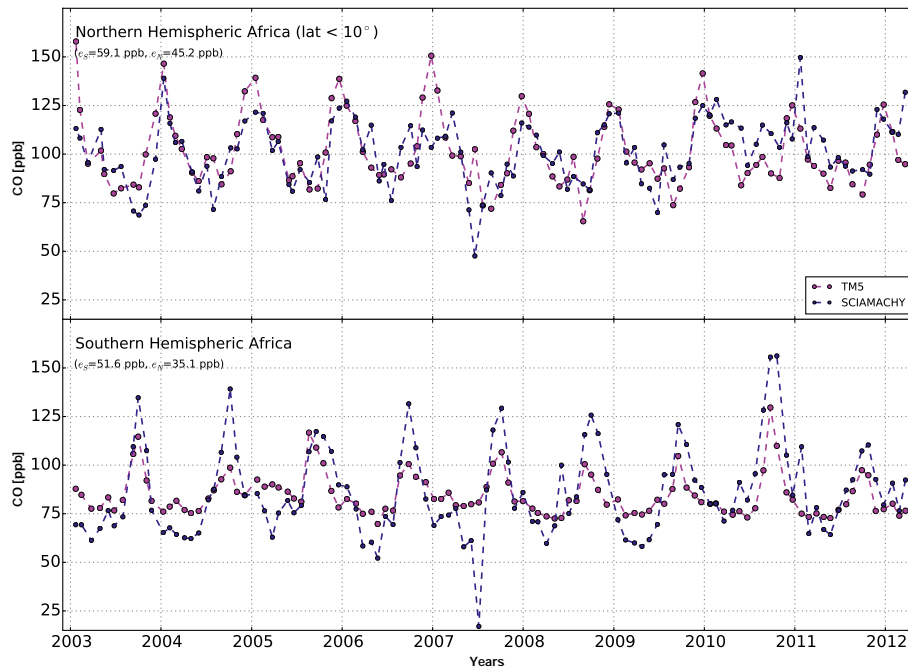
Figure 12. Time series of SCIAMACHY CO wet air column averaged mixing ratios (blue) over northern and southern hemispheric Africa compared with the calculation of the TM5 model (pink); 30-day medians are shown.

the validation of our data product. To ensure clear-sky conditions, SCIAMACHY observations are filtered strictly employing the onboard polarisation measurement device of the same instrument (SPICI algorithm).

The full-mission data set is validated with ground-based FTIR measurements at 27 stations of the NDACC-IRWG and TCCON network and MOZAIC/IAGOS airborne measurements at 26 airports worldwide. Here, measurements of the NDACC-IRWG network cover the entire mission pe-

riod. TCCON measurements can only be used to validate the CO product in the later phase of the mission, whereas IAGOS/MOZAIC measurements are mainly available for the early years of the mission. For the validation, it is important to realise the main and principal limitation of the SCIAMACHY CO product, which is its high retrieval noise of individual CO columns. It varies between 30 ppb over high albedo scenes and more than 170 ppb over dark ground scenes with low signal-to-noise measurements. Con-

sequently, averaging of individual data points is essential for practical data usage. Hence, we base our validation on monthly median column abundances for the comparison with the FTIR measurement and instrument error weighted means for the comparison with MOZAIC/IAGOS airborne observations. Overall, we found a good agreement with TCCON measurements with only a global mean bias of $\bar{b} = -1.2$ ppb with a station-to-station bias variation of $\overline{\sigma} = 7.2$ ppb. The negative sign of the bias means that SCIAMACHY CO is biased low in comparison with TCCON. For the NDACC-IRWG network, we obtained a significant mean station bias $\bar{b} = -9.2$ ppb with $\overline{\sigma} = 8.1$ ppb. Moreover, for the IAGOS/MOZAIC measurements, we find a mean station bias of $\bar{b} = -6.4$ ppb with $\overline{\sigma} = 5.6$ ppb. We detected a small but significant bias trend of about 1.47 ± 0.25 ppb yr^{-1} in the SCIAMACHY data. Correcting this bias trend, the bias with the IAGOS/MOZAIC measurements becomes 2.5 ppb, which is within the uncertainty of the IAGOS/MOZAIC measurements. The bias between SCIAMACHY and NDACC-IRWG measurements becomes -8.4 ppb and with the TCCON measurements -4.6 ppb. A discrepancy of 3.8 ppb remains between the global biases with NDACC-IRWG and TCCON, which is confirmed by directly comparing NDACC-IRWG and TCCON measurements. There are some possible reasons why the NDACC-IRWG and TCCON retrievals differ in that magnitude. NDACC-IRWG retrievals are done from the 5 μm and TCCON from the same 2.3 μm spectral regions as SCIAMACHY using different retrieval approaches. A disagreement of the line parameters of this region can easily lead to differences and is under investigation. Further, the retrieval of the two networks are based on different isotopic lines. NDACC-IRWG is using two ^{13}CO and one ^{12}CO line while TCCON retrievals are solely based on ^{12}CO lines. Furthermore, TCCON retrievals are calibrated by scaling the retrieved CO columns to the ones obtained from simultaneous in situ measurements (aircraft sampling or AirCore measurements) which is not done with the NDACC-IRWG data. Both ground-based FTIR data sets are very valuable for satellite validation, although for the validation of future satellite missions, like the Sentinel 5 Precursor (S5-P) mission to be launched in 2016, it is desirable to improve the comparability of NDACC-IRWG and TCCON measurements.

Finally, to demonstrate potential data use, we showed the seasonal cycle of biomass burning events in central Africa. Averaging the entire mission data set, the biomass burning area can be detected with good spatial resolution. On the other hand, the monthly median SCIAMACHY CO fields averaged over the northern and southern parts of central Africa, reflect the spatial and temporal variability of biomass burning events in this region, in good agreement with the global chemical transport model TM5.

This study represents the first application of the retrieval algorithm SICOR, which was developed for the operational data processing of the S5-P mission on real measurements of the shortwave infrared spectral range. Using the same retrieval approach for both satellite instruments will make the CO data sets of both missions more compatible, which is highly desirable from the perspective of long-term atmospheric monitoring. In a follow-up study, we will focus on extending the presented CO data set to SCIAMACHY ocean measurements.
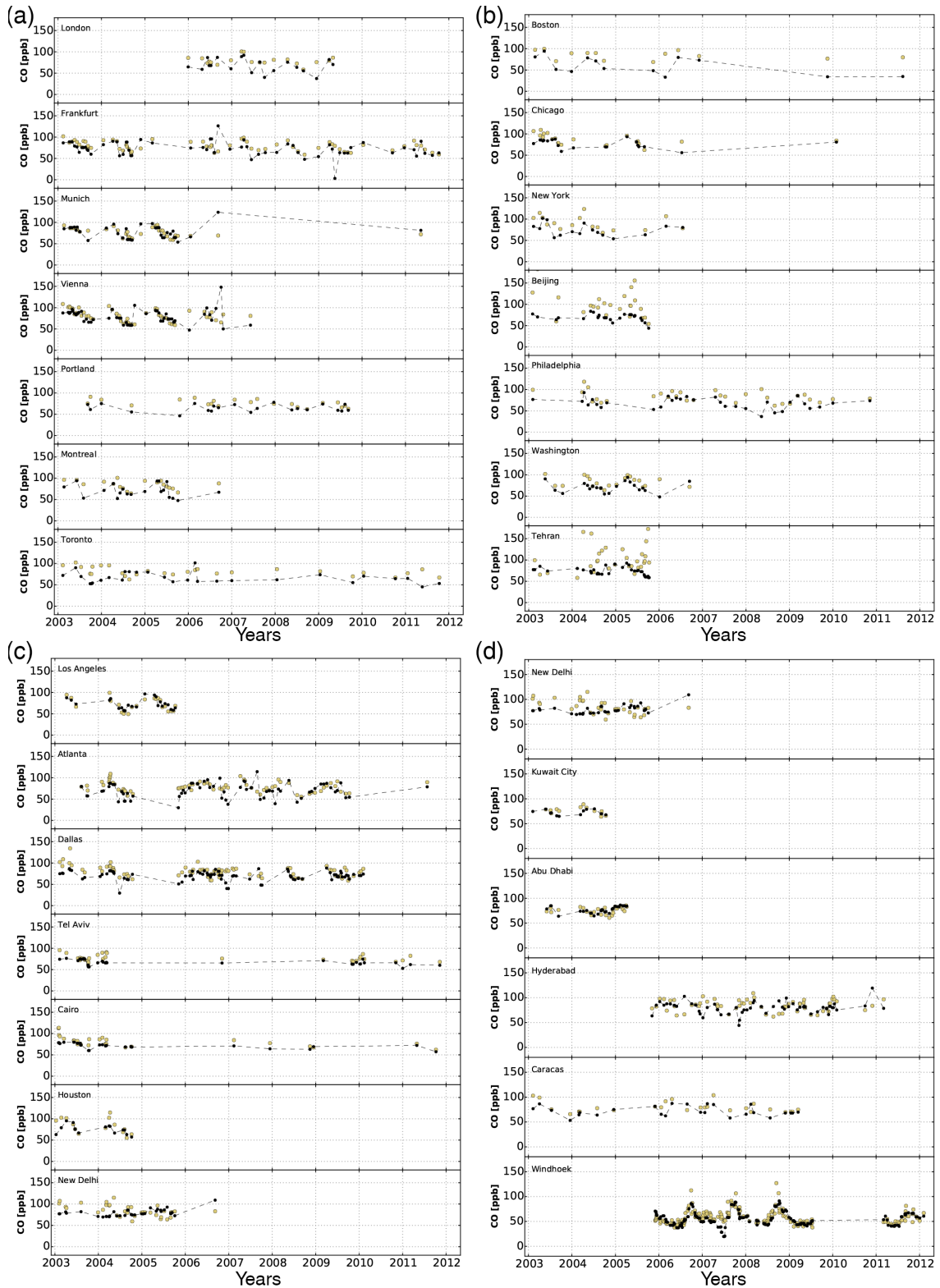
Appendix A

Figure A1. As Fig. 6, but for MOZAIC/IAGOS measurements indicated in yellow.

Edited by: H. Worden

References

Blumenstock, T., Hase, F., Schneider, M., García, O., and Sepúlveda., E.: TCCON Data from Izana, Tenerife, Spain, Release GGG2014R0, TCCON data archive, hosted by the Carbon Dioxide Information Analysis Center, Oak Ridge National Laboratory, Oak Ridge, TN, USA, doi:10.14291/tccon.ggg2014.izana01.R0/1149295, 2014.

Borsdorff, T., Hasekamp, O. P., Wassmann, A., and Landgraf, J.: Insights into Tikhonov regularization: application to trace gas column retrieval and the efficient calculation of total column averaging kernels, Atmos. Meas. Tech., 7, 523–535, doi:10.5194/amt-7-523-2014, 2014.

Bovensmann, H., Burrows, J. P., Buchwitz, M., Frerick, J., Noël, S., Rozanov, V. V., Chance, K. V., and Goede, A. P. H.: SCIAMACHY: mission objectives and measurement modes, J. Atmos. Sci., 56, 127–150, doi:10.1175/1520-0469(1999)056<0127:SMOAMM>2.0.CO;2, 1999.

Buchwitz, M., de Beek, R., Bramstedt, K., Noël, S., Bovensmann, H., and Burrows, J. P.: Global carbon monoxide as retrieved from SCIAMACHY by WFM-DOAS, Atmos. Chem. Phys., 4, 1945–1960, doi:10.5194/acp-4-1945-2004, 2004.

Buchwitz, M., Khlystova, I., Bovensmann, H., and Burrows, J. P.: Three years of global carbon monoxide from SCIAMACHY: comparison with MOPITT and first results related to the detection of enhanced CO over cities, Atmos. Chem. Phys., 7, 2399–2411, doi:10.5194/acp-7-2399-2007, 2007.

Daniel, J. S. and Solomon, S.: On the climate forcing of carbon monoxide, J. Geophys. Res., 103, 13249–13260, doi:10.1029/98JD00822, 1998.

de Laat, A. T. J., Gloudemans, A. M. S., Aben, I., and Schrijver, H.: Global evaluation of SCIAMACHY and MOPITT carbon monoxide column differences for 2004–2005, J. Geophys. Res.-Atmos., 115, D06307, doi:10.1029/2009JD012698, 2010a.

de Laat, A. T. J., Gloudemans, A. M. S., Schrijver, H., Aben, I., Nagahama, Y., Suzuki, K., Mahieu, E., Jones, N. B., Paton-Walsh, C., Deutscher, N. M., Griffith, D. W. T., De Mazière, M., Mittermeier, R. L., Fast, H., Notholt, J., Palm, M., Hawat, T., Blumen-

stock, T., Hase, F., Schneider, M., Rinsland, C., Dzhola, A. V., Grechko, E. I., Poberovskii, A. M., Makarova, M. V., Mellqvist, J., Strandberg, A., Sussmann, R., Borsdorff, T., and Rettinger, M.: Validation of five years (2003–2007) of SCIAMACHY CO total column measurements using ground-based spectrometer observations, Atmos. Meas. Tech., 3, 1457–1471, doi:10.5194/amt-3-1457-2010, 2010b.

de Laat, A. T. J., Dijkstra, R., Schrijver, H., Nédélec, P., and Aben, I.: Validation of six years of SCIAMACHY carbon monoxide observations using MOZAIC CO profile measurements, Atmos. Meas. Tech., 5, 2133–2142, doi:10.5194/amt-5-2133-2012, 2012.

de Laat, A. T. J., Aben, I., Deeter, M., Nédélec, P., Eskes, H., Attié, J.-L., Ricaud, P., Abida, R., El Amraoui, L., and Landgraf, J.: Validation of nine years of MOPITT V5 NIR using MOZAIC/IAGOS measurements: biases and long-term stability, Atmos. Meas. Tech., 7, 3783–3799, doi:10.5194/amt-7-3783-2014, 2014.

Dee, D. P., Uppala, S. M., Simmons, A. J., Berrisford, P., Poli, P., Kobayashi, S., Andrae, U., Balmaseda, M. A., Balsamo, G., Bauer, P., Bechtold, P., Beljaars, A. C. M., van de Berg, L., Bidlot, J., Bormann, N., Delsol, C., Dragani, R., Fuentes, M., Geer, A. J., Haimberger, L., Healy, S. B., Hersbach, H., Hólm, E. V., Isaksen, L., Kållberg, P., Köhler, M., Matricardi, M., McNally, A. P., Monge-Sanz, B. M., Morcrette, J.-J., Park, B.-K., Peubey, C., de Rosnay, P., Tavolato, C., Thépaut, J.-N., and Vitart, F.: The ERA-Interim reanalysis: configuration and performance of the data assimilation system, Q. J. Roy. Meteor. Soc., 137, 553–597, doi:10.1002/qj.828, 2011.

Deeter, M. N., Emmons, L. K., Francis, G. L., Edwards, D. P., Gille, J. C., Warner, J. X., Khattatov, B., Ziskin, D., Lamarque, J.-F., Ho, S.-P., Yudin, V., Attié, J.-L., Packman, D., Chen, J., Mao, D., and Drummond, J. R.: Operational carbon monoxide retrieval algorithm and selected results for the MOPITT instrument, J. Geophys. Res., 108, 4399–4409, doi:10.1029/2002JD003186, 2003.

Deutscher, N., Notholt, J., Messerschmidt, J., Weinzierl, C., Warneke, T., Petri, C., Grupe, P., and Katrynski, K.: TCCON Data from Bialystok, Poland, Release GGG2014R0., TCCON data archive, hosted by the Carbon Dioxide Information Analysis Center, Oak Ridge National Laboratory, Oak Ridge, TN, USA, doi:10.14291/tccon.ggg2014.bialystok01.R0/1149277, 2014.

Farr, T. G., Rosen, P. A., Caro, E., Crippen, R., Duren, R., Hensley, S., Kobrick, M., Paller, M., Rodriguez, E., Roth, L., Seal, D., Shaffer, S., Shimada, J., Umland, J., Werner, M., Oskin, M., Burbank, D., and Alsdorf, D.: The Shuttle Radar Topography Mission, Rev. Geophys., 45, RG2004, doi:10.1029/2005RG000183, 2007.

Frankenberg, C., Platt, U., and Wagner, T.: Retrieval of CO from SCIAMACHY onboard ENVISAT: detection of strongly polluted areas and seasonal patterns in global CO abundances, Atmos. Chem. Phys., 5, 1639–1644, doi:10.5194/acp-5-1639-2005, 2005.

Gimeno García, S., Schreier, F., Lichtenberg, G., and Slijkhuis, S.: Near infrared nadir retrieval of vertical column densities: methodology and application to SCIAMACHY, Atmos. Meas. Tech., 4, 2633–2657, doi:10.5194/amt-4-2633-2011, 2011.

Gloudemans, A. M. S., Schrijver, H., Kleipool, Q., van den Broek, M. M. P., Straume, A. G., Lichtenberg, G., van Hees, R. M.,

Aben, I., and Meirink, J. F.: The impact of SCIAMACHY near-infrared instrument calibration on CH_4 and CO total columns, Atmos. Chem. Phys., 5, 2369–2383, doi:10.5194/acp-5-2369-2005, 2005.

Gloudemans, A. M. S., Krol, M. C., Meirink, J. F., de Laat, A. T. J., van der Werf, G. R., Schrijver, H., van den Broek, M. M. P., and Aben, I.: Evidence for long-range transport of carbon monoxide in the Southern Hemisphere from SCIAMACHY observations, Geophys. Res. Let., 33, L16807, doi:10.1029/2006GL026804, 2006.

Gloudemans, A. M. S., Schrijver, H., Hasekamp, O. P., and Aben, I.: Error analysis for CO and CH_4 total column retrievals from SCIAMACHY 2.3 μm spectra, Atmos. Chem. Phys., 8, 3999–4017, doi:10.5194/acp-8-3999-2008, 2008.

Gloudemans, A. M. S., de Laat, A. T. J., Schrijver, H., Aben, I., Meirink, J. F., and van der Werf, G. R.: SCIAMACHY CO over land and oceans: 2003–2007 interannual variability, Atmos. Chem. Phys., 9, 3799–3813, doi:10.5194/acp-9-3799-2009, 2009.

Griffith, D. W. T., Deutscher, N., Velazco, V. A., Wennberg, P. O., Yavin, Y., Aleks, G. K., Washenfelder, R., Toon, G. C., Blavier, J.-F., Murphy, C., Jones, N., Kettlewell, G., Connor, B., Macatangay, R., Roehl, C., Ryczek, M., Glowacki, J., Culgan, T., and Bryant, G.: TCCON Data from Darwin, Australia, Release GGG2014R0., TCCON data archive, hosted by the Carbon Dioxide Information Analysis Center, Oak Ridge National Laboratory, Oak Ridge, TN, USA, doi:10.14291/tccon.ggg2014.darwin01.R0/1149290, 2014a.

Griffith, D. W. T., Velazco, V. A., Deutscher, N., Murphy, C., Jones, N., Wilson, S., Macatangay, R., Kettlewell, G., Buchholz, R. R., and Riggenbach, M.: TCCON Data from Wollongong, Australia, Release GGG2014R0., TCCON data archive, hosted by the Carbon Dioxide Information Analysis Center, Oak Ridge National Laboratory, Oak Ridge, TN, USA, doi:10.14291/tccon.ggg2014.wollongong01.R0/1149291, 2014b.

Holloway, T., Levy, H., and Kasibhatla, P.: Global distribution of carbon monoxide, J. Geophys. Res., 105, 12123–12148, doi:10.1029/1999JD901173, 2000.

Inness, A., Baier, F., Benedetti, A., Bouarar, I., Chabrillat, S., Clark, H., Clerbaux, C., Coheur, P., Engelen, R. J., Errera, Q., Flemming, J., George, M., Granier, C., Hadji-Lazaro, J., Huijnen, V., Hurtmans, D., Jones, L., Kaiser, J. W., Kapsomenakis, J., Lefever, K., Leitão, J., Razinger, M., Richter, A., Schultz, M. G., Simmons, A. J., Suttie, M., Stein, O., Thépaut, J.-N., Thouret, V., Vrekoussis, M., Zerefos, C., and the MACC team: The MACC reanalysis: an 8 yr data set of atmospheric composition, Atmos. Chem. Phys., 13, 4073–4109, doi:10.5194/acp-13-4073-2013, 2013.

Inness, A., Benedetti, A., Flemming, J., Huijnen, V., Kaiser, J. W., Parrington, M., and Remy, S.: The ENSO signal in atmospheric composition fields: emission-driven versus dynamically induced changes, Atmos. Chem. Phys., 15, 9083–9097, doi:10.5194/acp-15-9083-2015, 2015.

Jenouvrier, A., Daumont, L., Régalia-Jarlot, L., Tyuterev, V. G., Carleer, M., Vandaele, A. C., Mikhailenko, S., and Fally, S.: Fourier transform measurements of water vapor line parameters in the 4200 6600 cm^{-1} region, J. Quant. Spectrosc. Ra., 105, 326–355, doi:10.1016/j.jqsrt.2006.11.007, 2007.

Kawakami, S., Ohyama, H., Arai, K., Okumura, H., Taura, C., Fukamachi, T., and Sakashita, M.: TCCON Data from Saga, Japan, Release GGG2014R0., TCCON Data Archive, hosted by the Carbon Dioxide Information Analysis Center, Oak Ridge National Laboratory, Oak Ridge, TN, USA, doi:10.14291/tccon.ggg2014.saga01.R0/1149283, 2014.

Kivi, R., Heikkinen, P., and Kyro, E.: TCCON Data from Sodankyla, Finland, Release GGG2014R0., TCCON Data Archive, hosted by the Carbon Dioxide Information Analysis Center, Oak Ridge National Laboratory, Oak Ridge, TN, USA, doi:10.14291/tccon.ggg2014.sodankyla01.R0/1149280, 2014.

Krijger, J. M., Aben, I., and Schrijver, H.: Distinction between clouds and ice/snow covered surfaces in the identification of cloud-free observations using SCIAMACHY PMDs, Atmos. Chem. Phys., 5, 2729–2738, doi:10.5194/acp-5-2729-2005, 2005.

Levelt, P. F., Veefkind, J. P., Kerridge, B. J., Siddans, R., de Leeuw, G., Remedios, J., and Coheur, P. F.: Observation Techniques and Mission Concepts for Atmospheric Chemistry (CAMELOT), Report 20533/07NL/HE, European Space Agency, Noordwijk, the Netherlands, 2009.

Logan, J. A., Prather, M. J., Wofsy, S. C., and McElroy, M. B.: Tropospheric chemistry – a global perspective, J. Geophys. Res., 86, 7210–7254, doi:10.1029/JC086iC08p07210, 1981.

Marenco, A., Thouret, V., NéDéLec, P., Smit, H., Helten, M., Kley, D., Karcher, F., Simon, P., Law, K., Pyle, J., Poschmann, G., von Wrede, R., Hume, C., and Cook, T.: Measurement of ozone and water vapor by Airbus in-service aircraft: the MOZAIC airborne program, an overview, J. Geophys. Res., 103, 25631, doi:10.1029/98JD00977, 1998.

Maziere, M. D., Desmet, F., Hermans, C., Scolas, F., Kumps, N., Metzger, J.-M., Duflot, V., and Cammas, J.-P.: TCCON Data from Reunion Island (La Reunion), France, Release GGG2014R0, TCCON Data Archive, hosted by the Carbon Dioxide Information Analysis Center, Oak Ridge National Laboratory, Oak Ridge, TN, USA, doi:10.14291/tccon.ggg2014.reunion01.R0/1149288, 2014.

McMillan, W., Barnet, C., Strow, L., Chahine, M. T., McCourt, M. L., Warner, J. X., Novelli, P. C., Korontzi, S., Maddy, E. S., and Datta, S.: Daily global maps of carbon monoxide from NASA's Atmospheric Infrared Sounder, Geophys. Res. Lett., 32, L11801, doi:10.1029/2004GL021821, 2005.

Morino, I., Matsuzaki, T., Ikegami, H., and Shishime, A.: TCCON Data from Tsukuba, Ibaraki, Japan, 125HR, Release GGG2014R0, TCCON Data Archive, hosted by the Carbon Dioxide Information Analysis Center, Oak Ridge National Laboratory, Oak Ridge, TN, USA, doi:10.14291/tccon.ggg2014.tsukuba02.R0/1149301, 2014.

Nedelec, P., Cammas, J.-P., Thouret, V., Athier, G., Cousin, J.-M., Legrand, C., Abonnel, C., Lecoeur, F., Cayez, G., and Marizy, C.: An improved infrared carbon monoxide analyser for routine measurements aboard commercial Airbus aircraft: technical validation and first scientific results of the MOZAIC III programme, Atmos. Chem. Phys., 3, 1551–1564, doi:10.5194/acp-3-1551-2003, 2003.

Nédélec, P., Blot, R., Boulanger, D., Athier, G., Cousin, J.-M., Gautron, B., Petzold, A., Volz-Thomas, A., and Thouret, V.: Instrumentation on commercial aircraft for monitoring the atmospheric composition on a global scale: the IAGOS system, tech-

nical overview of ozone and carbon monoxide measurements, Tellus B, 67, 27791, doi:10.3402/tellusb.v67.27791, 2015.

NOAA: US Standard Atmosphere, 1976, Report NOAA-S/T76-1562, National Oceanic and Atmospheric Administration, Washington, DC, US Gov. Printing Office, 243 pp., 1976.

Predoi-Cross, A., Brawley-Tremblay, M., Brown, L. R., Devi, V. M., and Benner, D. C.: Multispectrum analysis of $^{12}CH_4$ from 4100 to 4635 cm^{-1}: II. Air-broadening coefficients (widths and shifts), J. Mol. Spectrosc., 236, 201–215, doi:10.1016/j.jms.2006.01.013, 2006.

Rinsland, C. P., Luo, M., Logan, J. A., Beer, R., Worden, H., Kulawik, S. S., Rider, D., Osterman, G., Gunson, M., Eldering, A., Goldman, A., Shephard, M., Clough, S. A., Rodgers, C., Lampel, M., and Chiou, L.: Nadir measurements of carbon monoxide distributions by the Tropospheric Emission Spectrometer instrument onboard the Aura Spacecraft: Overview of analysis approach and examples of initial results, Geophys. Res. Lett., 33, L22806, doi:10.1029/2006GL027000, 2006.

Rodgers, C. D.: Inverse Methods for Atmospheric Sounding: Theory and Practice, Series on atmospheric, oceanic and planetary physics, World Scientific, Singapore, ISBN: 9789810227401, 2000.

Rothman, L. S., Jacquemart, D., Barbe, A., Chris Benner, D., Birk, M., Brown, L. R., Carleer, M. R., Chackerian, C., Chance, K., Coudert, L. H., Dana, V., Devi, V. M., Flaud, J.-M., Gamache, R. R., Goldman, A., Hartmann, J.-M., Jucks, K. W., Maki, A. G., Mandin, J.-Y., Massie, S. T., Orphal, J., Perrin, A., Rinsland, C. P., Smith, M. A. H., Tennyson, J., Tolchenov, R. N., Toth, R. A., Vander Auwera, J., Varanasi, P., and Wagner, G.: The HITRAN 2004 molecular spectroscopic database, J. Quant. Spectrosc. Ra., 96, 139–204, doi:10.1016/j.jqsrt.2004.10.008, 2005.

Schrijver, H.: Spectral Calibration of SCIAMACHY Channels 7 and 8 Using Gas Cell Absorption Spectra, Tech. Rep. SRON-EOS-HS-99001, issue 1, SRON, Utrecht, the Netherlands, 1999.

Schrijver, H.: Line Profiles for SCIAMACHY Channels 7 and 8 Derived from Gas Cell Absorption Spectra, Tech. Rep. SRON-EOS-HS-00002, issue 1, SRON, Utrecht, the Netherlands, 2000a.

Schrijver, H.: New Spectral Calibration of SCIAMACHY Channels 7 and 8 Using Gas Cell Absorption Spectra, Tech. Rep. SRON-EOS-HS-00001, issue 1, SRON, Utrecht, the Netherlands, 2000b.

Schrijver, H.: Slit Functions for SCIAMACHY Channel 7 and 8, Tech. Rep. SRON-EOS-HS-01001, issue 1, SRON, Utrecht, the Netherlands, 2001a.

Schrijver, H.: Further on Spectral Calibration of SCIAMACHY Channels 7 and 8, Tech. Rep. SRON-EOS-HS-01002, issue 1, SRON, Utrecht, the Netherlands, 2001b.

Seiler, W. and Fishman, J.: The distribution of carbon monoxide and ozone in the free troposphere, J. Geophys. Res., 86, 7255–7265, doi:10.1029/JC086iC08p07255, 1981.

Sherlock, V., Connor, B., Robinson, J., Shiona, H., Smale, D., and Pollard, D.: TCCON Data from Lauder, New Zealand, 120HR, Release GGG2014R0, TCCON Data Archive, hosted by the Carbon Dioxide Information Analysis Center, Oak Ridge National Laboratory, Oak Ridge, TN, USA, doi:10.14291/tccon.ggg2014.lauder01.R0/1149293, 2014.

Spivakovsky, C. M., Logan, J. A., Montzka, S. A., Balkanski, Y. J., Foreman-Fowler, M., Jones, D. B. A., Horowitz, L. W.,

Fusco, A. C., Brenninkmeijer, C. A. M., Prather, M. J., Wofsy, S. C., and McElroy, M. B.: Three-dimensional climatological distribution of tropospheric OH: update and evaluation, J. Geophys. Res., 105, 8931–8980, doi:10.1029/1999JD901006, 2000.

Strong, K., Mendonca, J., Weaver, D., Fogal, P., Drummond, J., Batchelor, R., and Lindenmaier, R.: TCCON Data from Eureka, Canada, Release GGG2014R0, TCCON Data Archive, hosted by the Carbon Dioxide Information Analysis Center, Oak Ridge National Laboratory, Oak Ridge, TN, USA, doi:10.14291/tccon.ggg2014.eureka01.R0/1149271, 2014.

Sussmann, R. and Rettinger, M.: TCCON Data from Garmisch, Germany, Release GGG2014R0, TCCON Data Archive, hosted by the Carbon Dioxide Information Analysis Center, Oak Ridge National Laboratory, Oak Ridge, TN, USA, doi:10.14291/tccon.ggg2014.garmisch01.R0/1149299, 2014.

Turquety, S., Hadji-Lazaro, J., Clerbaux, C., Hauglustaine, D. A., Clough, S. A., Cassé, V., Schlüssel, P., and Mégie, G.: Operational trace gas retrieval algorithm for the Infrared Atmospheric Sounding Interferometer, J. Geophys. Res., 109, D21301, doi:10.1029/2004JD004821, 2004.

Vidot, J., Landgraf, J., Hasekamp, O., Butz, A., Galli, A., Tol, P., and Aben, I.: Carbon monoxide from shortwave infrared reflectance measurements: a new retrieval approach for clear sky and partially cloudy atmospheres, the Sentinel Missions – new opportunities for science, Remote Sens. Environ., 120, 255–266, 2012.

Warneke, T., Messerschmidt, J., Notholt, J., Weinzierl, C., Deutscher, N., Petri, C., Grupe, P., Vuillemin, C., Truong, F., Schmidt, M., Ramonet, M., and Parmentier, E.: TCCON Data from Orleans, France, Release GGG2014R0, TCCON Data Archive, hosted by the Carbon Dioxide Information Analysis Center, Oak Ridge National Laboratory, Oak Ridge, TN, USA, doi:10.14291/tccon.ggg2014.orleans01.R0/1149276, 2014.

Wennberg, P. O., Roehl, C., Blavier, J.-F., Wunch, D., Landeros, J., and Allen, N.: TCCON Data from Jet Propulsion Laboratory, Pasadena, California, USA, Release GGG2014R0, TCCON Data Archive, hosted by the Carbon Dioxide Information Analysis Center, Oak Ridge National Laboratory, Oak Ridge, TN, USA, doi:10.14291/tccon.ggg2014.jpl02.R0/1149297, 2014a.

Wennberg, P. O., Roehl, C., Wunch, D., Toon, G. C., Blavier, J.-F., Washenfelder, R., Keppel-Aleks, G., Allen, N., and Ayers, J.: TCCON Data from Park Falls, Wisconsin, USA, Release GGG2014R0, TCCON Data Archive, hosted by the Carbon Dioxide Information Analysis Center, Oak Ridge National Laboratory, Oak Ridge, TN, USA, doi:10.14291/tccon.ggg2014.parkfalls01.R0/1149161, 2014b.

Wennberg, P. O., Wunch, D., Roehl, C., Blavier, J.-F., Toon, G. C., and Allen, N.: TCCON Data from California Institute of Technology, Pasadena, California, USA, Release GGG2014R1, TCCON Data Archive, hosted by the Carbon Dioxide Information Analysis Center, Oak Ridge National Laboratory, Oak Ridge, TN, USA, doi:10.14291/tccon.ggg2014.pasadena01.R1/1182415, 2014c.

Wennberg, P. O., Wunch, D., Roehl, C., Blavier, J.-F., Toon, G. C., Allen, N., Dowell, P., Teske, K., Martin, C., and Martin, J.: TCCON Data from Lamont, Oklahoma, USA, Release GGG2014R0, TCCON Data Archive, hosted by the Carbon Dioxide Information Analysis Center,

Oak Ridge National Laboratory, Oak Ridge, TN, USA, doi:10.14291/tccon.ggg2014.lamont01.R0/1149159, 2014d.

Wennberg, P. O., Wunch, D., Yavin, Y., Toon, G. C., Blavier, J.-F., Allen, N., and Keppel-Aleks, G.: TCCON Data from Jet Propulsion Laboratory, Pasadena, California, USA, Release GGG2014R0, TCCON Data Archive, hosted by the Carbon Dioxide Information Analysis Center, Oak Ridge National Laboratory, Oak Ridge, TN, USA, doi:10.14291/tccon.ggg2014.jpl01.R0/1149163, 2014e.

Williams, J. E., van Velthoven, P. F. J., and Brenninkmeijer, C. A. M.: Quantifying the uncertainty in simulating global tropospheric composition due to the variability in global emission estimates of Biogenic Volatile Organic Compounds, Atmos. Chem. Phys., 13, 2857–2891, doi:10.5194/acp-13-2857-2013, 2013.

Williams, J. E., Le Bras, G., Kukui, A., Ziereis, H., and Brenninkmeijer, C. A. M.: The impact of the chemical production of methyl nitrate from the $NO + CH_3O_2$ reaction on the global distributions of alkyl nitrates, nitrogen oxides and tropospheric ozone: a global modelling study, Atmos. Chem. Phys., 14, 2363–2382, doi:10.5194/acp-14-2363-2014, 2014.

Wofsy, S. C.: HIAPER Pole-to-Pole Observations (HIPPO): fine-grained, global-scale measurements of climatically important atmospheric gases and aerosols, Philos. T. R. Soc. A, 369, 2073–2086, doi:10.1098/rsta.2010.0313, 2011.

Wofsy, S., Daube, B., Jimenez, R., Kort, E., Pittman, J., Park, S., Commane, R., Xiang, B., Santoni, G., Jacob, D., Fisher, J., Pickett-Heaps, C., Wang, H., Wecht, K., Wang, Q.-Q., Stephens, B., Shertz, S., Watt, A., Romashkin, P., Campos, T., Haggerty, J., Cooper, W., Rogers, D., Beaton, S., Hendershot, R., Elkins, J., Fahey, D., Gao, R., Moore, F., Montzka, S., Schwarz, J., Perring, A., Hurst, D., Miller, B., Sweeney, C., Oltmans, S., Nance, D., Hintsa, E., Dutton, G., Watts, L., Spackman, J., Rosenlof, K., Ray, E., Hall, B., Zondlo, M., Diao, M., Keeling, R., Bent, J., Atlas, E., Lueb, R., and Mahoney, M.: HIPPO Merged 10-second Meteorology, Atmospheric Chemistry, Aerosol Data (R_20121129), Carbon Dioxide Information Analysis Center, Oak Ridge National Laboratory, Oak Ridge, TN, USA, doi:10.3334/CDIAC/hippo_010 (Release 20121129), 2012.

Wunch, D., Toon, G. C., Wennberg, P. O., Wofsy, S. C., Stephens, B. B., Fischer, M. L., Uchino, O., Abshire, J. B., Bernath, P., Biraud, S. C., Blavier, J.-F. L., Boone, C., Bowman, K. P., Browell, E. V., Campos, T., Connor, B. J., Daube, B. C., Deutscher, N. M., Diao, M., Elkins, J. W., Gerbig, C., Gottlieb, E., Griffith, D. W. T., Hurst, D. F., Jiménez, R., Keppel-Aleks, G., Kort, E. A., Macatangay, R., Machida, T., Matsueda, H., Moore, F., Morino, I., Park, S., Robinson, J., Roehl, C. M., Sawa, Y., Sherlock, V., Sweeney, C., Tanaka, T., and Zondlo, M. A.: Calibration of the Total Carbon Column Observing Network using aircraft profile data, Atmos. Meas. Tech., 3, 1351–1362, doi:10.5194/amt-3-1351-2010, 2010.

Wunch, D., Wennberg, P. O., Toon, G. C., Connor, B. J., Fisher, B., Osterman, G. B., Frankenberg, C., Mandrake, L., O'Dell, C., Ahonen, P., Biraud, S. C., Castano, R., Cressie, N., Crisp, D., Deutscher, N. M., Eldering, A., Fisher, M. L., Griffith, D. W. T., Gunson, M., Heikkinen, P., Keppel-Aleks, G., Kyrö, E., Lindenmaier, R., Macatangay, R., Mendonca, J., Messerschmidt, J., Miller, C. E., Morino, I., Notholt, J., Oyafuso, F. A., Rettinger, M., Robinson, J., Roehl, C. M., Salawitch, R. J., Sherlock, V., Strong, K., Sussmann, R., Tanaka, T., Thompson, D. R., Uchino, O., Warneke, T., and Wofsy, S. C.: A method for evaluating bias in global measurements of CO_2 total columns from space, Atmos. Chem. Phys., 11, 12317–12337, doi:10.5194/acp-11-12317-2011, 2011.

Yurganov, L. N., Blumenstock, T., Grechko, E. I., Hase, F., Hyer, E. J., Kasischke, E. S., Koike, M., Kondo, Y., Kramer, I., Leung, F.-Y., Mahieu, E., Mellqvist, J., Notholt, J., Novelli, P. C., Rinsland, C. P., Scheel, H. E., Schulz, A., Strandberg, A., Sussmann, R., Tanimoto, H., Velazco, V., Zander, R., and Zhao, Y.: A quantitative assessment of the 1998 carbon monoxide emission anomaly in the Northern Hemisphere based on total column and surface concentration measurements, J. Geophys. Res., 109, D15305, doi:10.1029/2004JD004559, 2004.

Yurganov, L. N., Duchatelet, P., Dzhola, A. V., Edwards, D. P., Hase, F., Kramer, I., Mahieu, E., Mellqvist, J., Notholt, J., Novelli, P. C., Rockmann, A., Scheel, H. E., Schneider, M., Schulz, A., Strandberg, A., Sussmann, R., Tanimoto, H., Velazco, V., Drummond, J. R., and Gille, J. C.: Increased Northern Hemispheric carbon monoxide burden in the troposphere in 2002 and 2003 detected from the ground and from space, Atmos. Chem. Phys., 5, 563–573, doi:10.5194/acp-5-563-2005, 2005.